HEAT TRANSFER

IN

INDIRECT-HEAT AGITATED DRYER

TAKAO OHMORI

1984

HEAT TRANSFER IN INDIRECT-HEAT AGITATED DRYER

TAKAO OHMORI

1984

C O N T E N T S

CHAPTER 1

INTRODUCTION

The indirect-heat agitated dryer is defined as one
on which the housing enclosing the process is station-
ary, while the movement of the granular material is
accomplished by an internal mechanical agitator [16].
Heat required to dry material is transferred by conduc-
tion in this type of dryer. There are generally two
types in this dryer. We call one the "stationary
heating-plane type" and the other the "moving heating-
plane type". In the former, the steam-jacketed wall
of the dryer acts as a stationary heating plane and the
agitator serves to move the granular material over the
heating wall. In the latter, the agitator is hollow
with a heating medium flowing within it and the surface
of the agitator acts as a heating plane. The heating
plane moves in the granular bed.

This type of dryer can save energy use and can
prevent environmental pollution because of its high
thermal efficiency and minimal exhaust gas compared with
other types of dryers. High thermal efficiency is

mainly due to the conductive-heating. Minimal exhaust gas reduces the scale of the dust collector. Accordingly, this unit has been widely used recently in many fields: for example, in the drying of granular ores, chemicals, plastics, foods and so on. However, there is little basic information on the design of this type of dryer and it seems to depend mostly on the experience. Therefore, the main purposes of this study are to obtain data about the design and analysis of the heat transfer mechanism which controls the drying rate.

1-1 Historical Review

The heat transfer in the indirect-heat agitated dryer used here has not been reported. Therefore, this section treats the heat transfer between the heating plane and the granular material generally.

The heat transfer between the heating plane and the granular bed is one of the basic unit operation in the chemical engineering. Therefore, many studies on it have been reported so far. Some studies which had been already reported till 1966 were reviewed by Uhl and Root [26]. So this review is mainly concerned with the

investigations which had not been dealt with their review.

The heat transfer between the heating wall and the granular material flowing down vertically was studied by many investigators [2,3,25, for example]. In this case, the contact time between the heating wall and the granular material could be obtained precisely because it was easy to adjust the flow rate of the granular material. On the other hand, it was very difficult to determine the exact contact time in the other type of the experimental apparatus. Wunschmann and Schlünder [28] used the vertical cylindrical vessel with an internal mechanical agitator, in which the flat bottom plane was a heating plane. Lücke [12] measured the distribution of the local heat transfer coefficient in the circumferential direction in the horizontal cylindrical indirect-heat agitated dryer. Lehmberg et al. [11] treated the heat transfer in the horizontal cylinder without any internal agitator.

The heat transfer between the granular material and the heating plane submerged in it under the condition that there existed the relative velocity between them has been also published. Kurochkin [9,10] measured the

local heat transfer coefficient between the granular material and the heating cylinder or elliptical cylinder. Harakas and Beatty [5] studied the heat transfer from the submerged flat plate into the granular material in the vertical cylindrical vessel.

The heat transfer between the granular material and the heating plane submerged in the fluidized bed has been studied by many investigators [1,6,27,30, for example]. However, Gabor [4] might be only investigator who studied the same heat transfer under the condition that the gas, whose velocity was less than the minimum fluidization one, flowed through the bed. In his experiments, there did not exist the relative velocity between the heating plane and the granular bed.

Schlünder et al. [18∿24,28] have been investigating the heat transfer in this field theoretically and experimentally and proposed the "particle heat transfer model", which was partly revised by Mollekopf and Martin [14]. In this model, the point to be appreciated most is that he could interpret the existence of the heat transfer resistance at the interface between the heating plane and the granular bed physically and reasonably. Although the existence of this resistance was well known

widely, no reasonable explanation had been given and it was usually explained that there existed a gas film between the heating plane and the granular bed [3,25, for example]. Schlünder could succeed interpretting it by using the theory of the heat transfer under the vacuum. Therefore, it is not necessary to study this point.

However, the effect of the clearance between the heating plane and the agitator blade on the heat transfer was not taken into account quantitatively in his model. He introduced the "mixing number", which was an index indicating the mixing degree of the granular bed into his model. Then this variable was changed if the clearance was changed. But the physical meaning of this variable is not so clear and it can be thought that this point should be improved in his model.

1-2 Abstract of This Thesis

The main purposes of this study were to measure the heat transfer coefficient between the heating plane and the granular material in the indirect-heat agitated dryer and to propose the heat transfer model estimating

it by the analysis of the heat transfer mechanism.   In
Chapter 2, the heat transfer in the "stationary heating-
plane type" of the indirect-heat agitated dryer was
dealt with.   Chapter 3 treated the heat transfer in the
"moving heating-plane type" and Chapter 4 referred to
that in the new type of dryer, which was the "moving
heating-plane type" installed the device for the through-
flow gas.

In Chapter 2, the heat transfer coefficient between
the heating wall and the mechanically agitated granular
bed in the small indirect-heat agitated dryer was mea-
sured.   There was essentially a clearance between the
wall and the agitator blades in this type of dryer.
The effect of this clearance on the heat transfer was
very significant.   The heat transfer model considering
the effect of the clearance was proposed to correlate
the observed heat transfer coefficients.   The agreement
between the experimental and calculated heat transfer
coefficients was satisfactory.   Furthermore, it was con-
firmed that this model was also available even in the
case that the shape of particle was not spherical.

In Chapter 3, the heat transfer coefficient between
the granular bed and the heating plane submerged in it

was measured under the condition that there existed the relative velocity between them. The heating cylinder and the rotary coil were used as the "moving heating plane". In the former case, the heat flux generator (H.F.G.) was used in order to measure the heat transfer coefficient easily and quickly, which was especially prepared for this measurement by the author. The heat transfer model predicting the heat transfer coefficient in this case was proposed. The comparison between the experimental and calculated heat transfer coefficient showed fairly good agreement under the condition that an air pocket did not appear behind the heating cylinder.

In Chapter 4, the heat transfer coefficient between the granular bed and the heating plane submerged in it under the condition that there existed the relative velocity between them and that air flowed through the bed was measured. Blowing gas through the granular bed was one method solving the problem that the power consumption required for the agitation of the material was very large in the large indirect-heat agitated dryer. The through-flow gas also promotes the removal of the vapor generated in the granular bed and the mixing of the bulk material. The velocity of this through-flow gas was

less than the minimum fluidization velocity, otherwise
the advantage that exhaust gas was little in this type
of dryer would be lost. Therefore, this chapter dealt
with the effect of this through-flow gas, which had some
advantages mentioned above, on the heat transfer. The
heat flux generator (H.F.G.) was also used in order to
measure the heat transfer coefficient in this case.
The heat transfer model considering the effect of the
through-flow gas was proposed. The agreement between
the observed and calculated heat transfer coefficient
was fairly good. As the result of this work, it was
concluded that the effect of the through-flow gas on
the heat transfer coefficient was insignificant provid-
ing that its velocity was less than the minimum fluid-
ization velocity and that the relative velocity between
the heating cylinder and the granular bed was not so
small.

1-3 Publications on This Thesis

"Heat Transfer in an Indirect-Heat Agitated Dryer",
Chemical Engineering & Processing, 18, 149/155 (1984)

"Heat Transfer Coefficient between Heating Wall and
Agitated Granular Bed", "Drying'85", Hemisphere,
New York, to be published

"Heat Transfer from Submerged Body Moving in Granular
Bed", "Drying'85", Hemisphere, New York,
to be published

CHAPTER 2

HEAT TRANSFER BETWEEN STATIONARY HEATING WALL AND
MECHANICALLY AGITATED GRANULAR BED

2-1 Introduction

The heat transfer between the heating wall and the
mechanically agitated granular bed is an important proc-
ess in many industrial operations: for example, in the
drying, the desorption, the heat exchange, the catalytic
reaction and so on. The study described in this chapter
is concerned with the heat transfer in the indirect-heat
agitated dryer. As mentioned in the Chapter 1, there
are generally two types in this dryer: the "stationary
heating-plane type" and the "moving heating-plane type".
This chapter deals with the former. In this type, the
steam-jacketed wall of the dryer acts as a stationary
heating wall and the agitator serves to move the granu-
lar material over the heating wall.

There is essentially a clearance between the wall
and the agitator blade in this type of dryer. It is

noted that the effect of this clearance on the heat transfer is very significant. It becomes furthermore important to estimate quantitatively its effect on the heat transfer coefficient when the scale-up of the dryer is considered, because the width of the clearance can not be kept quite small as the shaft of the agitator may bend in the large scale dryer.

2-2 Theory and Model

It is considered that the heat transfer in this case consists of four mechanisms shown in Fig.2-1.

 1) wall-to-particle heat transfer
 2) heat conduction in packed bed
 3) heat convection by particle motion in bulk material
 4) heat transfer in clearance

1) wall-to-particle heat transfer
    It is well known that the heat transfer resistance exists at the interface between the heating plane and the granular bed. Schlünder called this the wall-to-particle heat transfer resistance and proposed the model
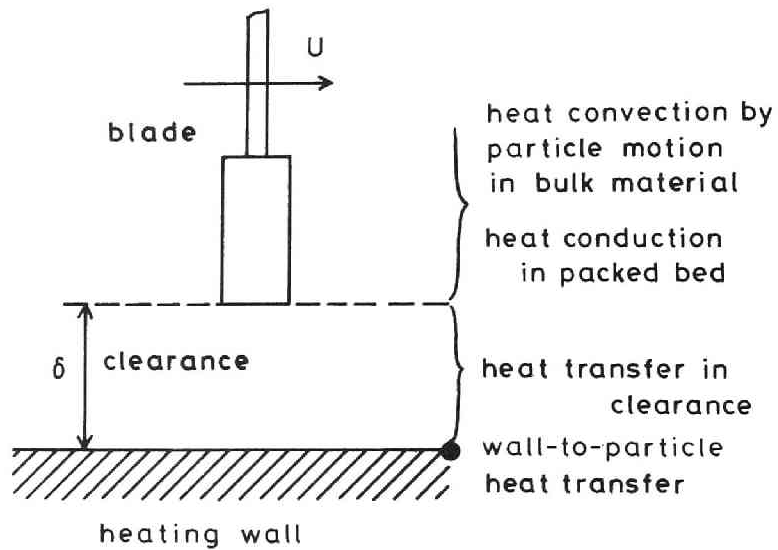
Fig.2-1 Heat transfer mechanism

estimating its value [21,22, for example]. That model
was partly revised by Mollekopf and Martin [14]. In
their model, the wall-to-particle heat transfer coeffi-
cient can be calculated by the following equations pro-
viding that the shape of paricle is spherical.

$$h_p = 4(\lambda_g/d_p)\{(1 + 2\sigma/d_p)\ln(1 + d_p/2\sigma) - 1\} \qquad (2-1)$$

$$\sigma = 2\frac{2-\gamma}{\gamma} \sqrt{2\pi RT/M} \; \frac{\lambda_g}{p(2c_{pg} - R/M)} \qquad (2-2)$$

$$h_s = \psi h_p + (1 - \psi)h_{2p} + h_R \qquad (2-3)$$

In these equations, h_p is the maximum achievable wall-to-particle heat transfer coefficient, h_s is the maximum achievable wall-to-particle-layer one, h_{2p} is one between the heating plane and the second layer particle from the plane and h_R is one by radiation. The surface coverage factor $\psi = 0.91$ if we assume that particles which are in direct contact with the heating wall are arranged in a hexagonal closest packing on it. The second and third terms in Eq.(2-3) are negligible in comparison with the first term so long as the pressure and temperature are atmospheric.

γ is an accomodation coefficient. In order to calculate its value for air, Martin [13] used the following empirical equation based on the experimental data of Reiter et al. [17]:

$$lg(1/\gamma - 1) = 0.6 - (1000/T + 1)/2.8 \qquad (2-4)$$

Using this equation, $\gamma = 0.85$ is obtained at 80°C, for example.

2) heat conduction in packed bed

The heat transfer coefficient of the heat conduc-

tion in packed bed is obtained by the "penetration model", in which packed bed is regarded as the homogeneous. The basic heat transfer equation is given as Eq.(2-5) [8].

$$\frac{\partial T}{\partial t} = \frac{\lambda_e}{c_{pm}\rho_b} \frac{\partial^2 T}{\partial x^2} \tag{2-5}$$

The instantaneous heat transfer coefficient is obtained as Eq.(2-9) by solving Eq.(2-5) under the initial and the boundary conditions shown in Eqs.(2-6)~(2-8).

$$T = T_b \quad \text{at} \quad t = 0 \tag{2-6}$$

$$T = T_w' \quad \text{at} \quad x = 0 \tag{2-7}$$

$$T = T_b \quad \text{at} \quad x = \infty \tag{2-8}$$

$$h_c = \sqrt{\lambda_e c_{pm}\rho_b \: / \: \pi t} \tag{2-9}$$

3) heat convection by particle motion in bulk material

As Schlünder mentioned [23], the heat convection by the particle motion has not been analysed quantitatively so far because the particle motion is not well known. However, its effect on the heat transfer can be neglected if the bulk material particles are mixed per-

fectly when the agitator blades scrape them. It is
noted that the present model is only applicable under
this condition.

4) heat transfer in clearance

    As shown in Fig.2-2(a), there may be some velocity
distribution of particles in this clearance. It is
difficult, however, to estimate this. Then we introduce
the hypothesis to this problem that there exists the
stationary particle layer, which has some effective
thickness δ_e, on the heating wall as shown in Fig.2-2
(b). According to this hypothesis, the heat transfer
resistance in this part is equal to δ_e/λ_e.
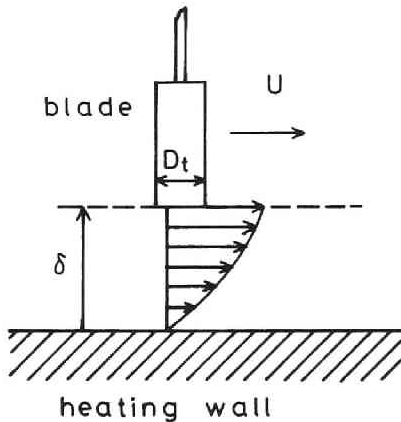
Fig.2-2(a)   Flow between
     agitator blade and
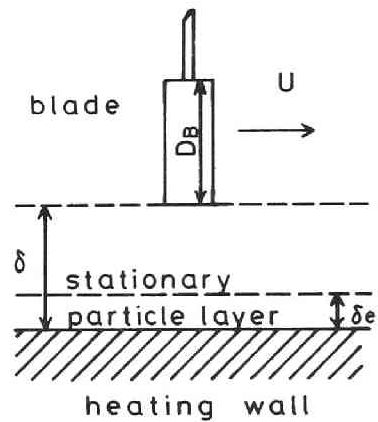   heating wall

Fig.2-2(b)   Stationary par-
     ticle layer

When those resistances mentioned above are connected in series to each other, we can get instantaneous heat transfer coefficient as follows.

$$h_i = 1 \ / \ (\ 1/h_s + \delta_e/\lambda_e + 1/h_c \ ) \tag{2-10}$$

Furthermore, it is assumed that the contact time in this case is equal to the interval of the scraping by the agitator blade. Therefore, the time-averaged heat transfer coefficient can be obtained by integrating Eq.(2-10) during this contact time.

$$
\begin{aligned}
h_w &= (\textstyle\int_0^\tau h_i \ dt) \ / \ \tau \\
&= 2h_s\lambda_e\{\sqrt{\pi\tau^\circ} - \ln(1+\sqrt{\pi\tau^\circ})\}/\{(\lambda_e+\delta_eh_s)\pi\tau^\circ\} \tag{2-11}
\end{aligned}
$$

$$\tau^\circ = h_s^2\lambda_e\tau/\{(\lambda_e + \delta_eh_s)^2 c_{pm}\rho_b\} \tag{2-12}$$

$$\tau = \pi(D - 2\delta) \ / \ U \tag{2-13}$$

Finally, we can calculate the heat transfer coefficient by Eqs.(2-1)~(2-3) and (2-11)~(2-13) if δ_e is known.

It can be considered that the effective thickness

depends on the width of the clearance δ, the particle diameter d_p, the fluidity of the granular bed, the thickness and the width of the agitator blade D_t, D_B, the velocity of the agitator blade U and the relative velocity between particles and the agitator blade along the lateral plane of the blade U_B (Fig.2-3).
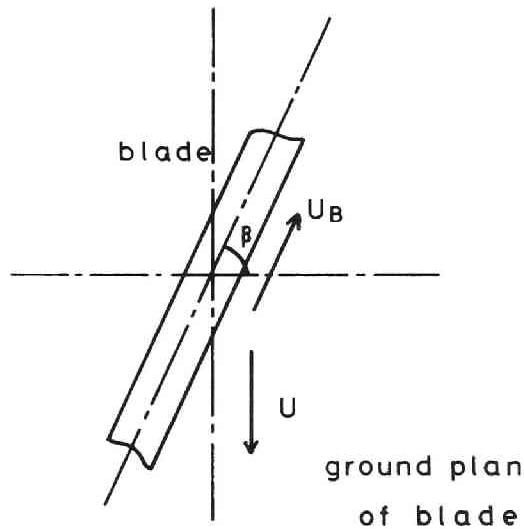

Fig.2-3 Relative velocity between blade and particles along lateral plane of blade

$$\delta_e = f(\delta, \ d_p, \ \mu, \ D_t, \ D_B, \ U, \ U_B) \qquad (2-14)$$

where μ is an angle of repose and it would be allowed to use as an index of the fluidity of the granular bed. However, μ, as well as D_t and D_B, did not vary so widely in the present experimental condition and besides the effects of D_t and D_B on δ_e might be insignificant unless they were so small. Therefore, we postulate that the effective thickness δ_e is described as the following form considering the extreme cases.

$$\delta/d_p \geqq 1 \quad : \quad \delta_e/d_p = 1 / (1/\xi + d_p/\delta) \qquad (2\text{-}15)$$

$$\xi = a(\delta/d_p - 1)^b/(U^c + dU_B{}^e) \qquad (2\text{-}16)$$

$$U_B = U \sin\beta \qquad (2\text{-}17)$$

$$0 \leqq \delta/d_p \leqq 1 \quad : \quad \delta_e = 0 \qquad (2\text{-}18)$$

where a, b, c, d and e are constant which should be determined by fitting the experimental data. The dimensionless variable ξ is an index indicating the variation of the effective thickness. If this value is equal to zero, $\delta_e = 0$. If it becomes infinite, $\delta_e = \delta$ as shown in Eq.(2-15). ξ naturally depends on the same factors

as δ_e. So this should depend on the dimensionless clearance δ/d_p. However, there can not be any stationary particle layer in the clearance if δ/d_p is less than unity. Then it is considered that ξ depends on (δ/d_p-1). Furthermore, it also depends on the circumferential velocity of the agitator U and the movement of particles over the clearance by the agitator blade, which can be described by the relative velocity between particles and the blade along the lateral plane of the blade U_B defined in Eq.(2-17). This is also an index indicating the effect of the angle of the blade to the moving direction of it. So the form of Eq.(2-16) are postulated. It is noted that the dimensions of U and U_B are meter by second in Eq.(2-16). In Eqs.(2-15)$\sim$(2-18), δ_e reaches zero if U becomes infinite and δ_e reaches δ if U becomes zero.

Through the experiments, a = 0.6, b = 0.5, c = 0.8, d = 3.5 and e = 0.45 were determined as described later in §2-4.

2-3 Experimentals

2-3-1 Apparatus

The experiments were carried out with a small hor-
izontal semi-cylindrical indirect-heat agitated dryer.
Its length is 80 cm and the diameter is 20 cm. A sche-
matic diagram of the experimental apparatus is shown in
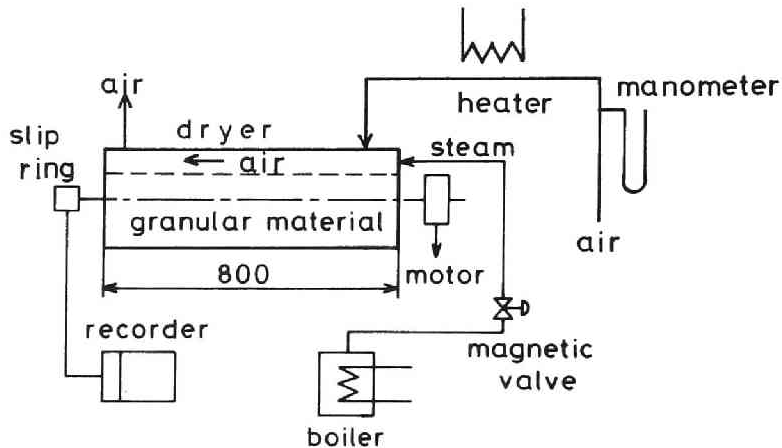Fig.2-4.

Fig.2-4 Schematic diagram of experimental apparatus

The temperature of the wall was kept at constant
by adjusting the steam flow rate. To avoid the heat
transfer from the granular bed to air over the bed sur-

face, hot air was blown over it. The heater for air
was controlled to keep the temperature of air equal to
that of the granular bed.

The temperature of the granular bed was measured at
two points in a radial direction to make sure that no
temperature distribution existed in that direction in
the bulk material. It had been confirmed beforehand
that there was no distribution in an axial direction.
The temperatures of both wall and air were measured at
four respective points and the averaged values were used
in the calculation of the heat transfer coefficient.
All temperatures were measured by thermocouples.

Two types of agitators were used in this experi-
ment. Those are shown in Figs.2-5 and 2-6. The former
shows the double spiral agitator, which consists of
discontinuous outer blades and continuous inner blades.
The width of the clearance between the wall and the
outer blades was changed by cutting down the blades from
0.7 mm to 5.6 mm. The angle of the blade to the moving
direction of it β is equal to 65° in this agitator.
The latter shows the flat bar agitator, which has four
outer blades and four inner blades. With this unit,
the width of the clearance can be arbitrarily varied by
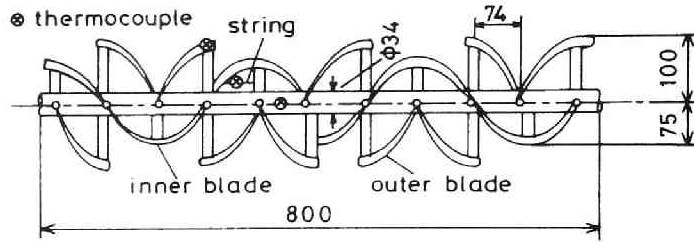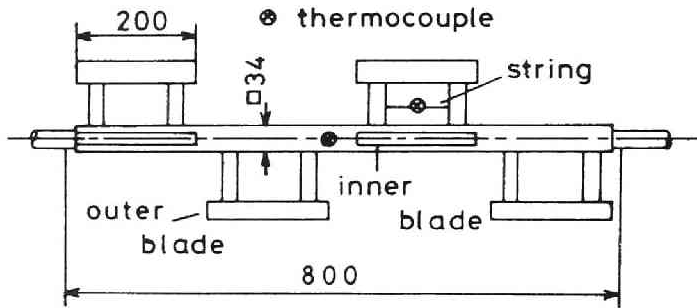
Fig.2-5 Double spiral agitator

Fig. 2-6 Flat bar agitator

adjusting the four outer blades. It was changed from
0.75 mm to 10.1 mm in the present experiments. The
angle β = 0° in this agitator.

2-3-2 Procedure

All the experiments were carried out under the condition that the temperature of the heating wall was constant.

The following equation can be obtained by the heat-balance in the system of both the granular bed and the agitator.

$$W_m c_{pm} \frac{dT_b}{dt} + W_{sh} c_{psh} \frac{dT_{sh}}{dt} = h_w A_w (T_w - T_b)$$
$$- h_a A_a (T_b - T_a) - Q_{loss} \quad (2-19)$$

where the first term on the left side is the heat accumulation rate of the granular bed, the second is that of the agitator, the first term on the right side is the heat transfer rate from the wall to the granular bed, the second is that from the bed to air over the bed surface and the third is other overall heat loss.

As mentioned above, T_a was equal to T_b in the present experimental condition. So the second term on the right side of Eq. (2-19) could be deleted. Furthermore, the third term Q_{loss} turned out to be negligible compared with the first as the result of the steady-state

heat transfer experiment. Finally, the time-avaraged
heat transfer coefficient can be calculated by the
following.

$$h_w = (W_m c_{pm} \frac{dT_b}{dt} + W_{sh} c_{psh} \frac{dT_{sh}}{dt})/\{A_w(T_w-T_b)\} \qquad (2-20)$$

The hold-up of the material was about 55%. Because,
the bulk material could not be mixed perfectly if the
hold-up was 100%. The heat transfer area A_w was deter-
mined by the observations.

After the dryer was filled with materials, the wall
was heated up to a given temperature by blowing steam
into the jacket and the rotational speed of the agitator
was set for a given one. Simultaneously, the flow of
air over the granular bed was started. Then the change
of the temperature of the bed and the shaft of the agi-
tator followed by the lapse of time were recorded.
After that, the heat transfer coefficient was calculated
by Eq.(2-20) using data obtained.

The possible overall error of the heat transfer
coefficient introduced by the present experimental pro-
cedure is estimated at about 20%.

2-3-3 Granular Materials

Five kinds of granular materials were used for the present experiments. Two of them were glass beads A and B, which had the same thermal properties and differed only in the particle size. The others were the spherical activated alumina, the spherical acrylic resin and the millet whose shape was flat oval. The properties of these granular materials are tabulated in Table 2-1. In this table, the effective thermal conductivities of the granular beds were measured by the Q.T.M. rapid thermal conductivity meter (manufactured by Showa Denko Co., Ltd.; QTM-D1) and the apparent densities of the bed of all and the specific heat at the constant pressure of the millet were also obtained by our measurements.

2-4 Results and Discussion

In Fig.2-7∿2-9, the observed heat transfer coefficients are plotted as a function of the circumferential velocity of the double spiral agitator. The observed heat transfer coefficients are plotted as a function of the circumferential velocity of the flat bar agitator

Table 2-1 Granular materials

Material	Shape	$d_p \times 10^3$	ρ_b	c_{pm}	λ_e
		[m]	[kg·m^{-3}]	[J·kg^{-1}·K^{-1}]	[W·m^{-1}·K^{-1}]
glass beads A	sphere	0.36	1450	853	0.203
glass beads B	sphere	1.1	1450	853	0.203
activated alumina	sphere	0.40	910	920	0.157
acrylic resin	sphere	0.57	690	1560	0.116
millet	flat oval	1.7	820	2300*	0.170

*measured under the condition dried up perfectly

in Figs.2-10 and 2-11. As the result of determining the
parameters in Eq.(2-16) to provide the best agreement
between data points and the curves calculated by the
present model, a = 0.6, b = 0.5, c = 0.8, d = 3.5 and
e = 0.45 were obtained. The calculated curves obtained
by the present model using those values are also shown
in Figs.2-7~2-11. The equations for calculating δ_e is
presented here again.

$\delta/d_p \geqq 1$: $\delta_e/d_p = 1 / (1/\xi + d_p/\delta)$ (2-15)

         $\xi = 0.6(\delta/d_p-1)^{0.5}/(U^{0.8}+3.5U_B^{0.45})$ (2-16)

         $U_B = U \sin\beta$ (2-17)

$0 \leqq \delta/d_p \leqq 1$: $\delta_e = 0$ (2-18)

         $0.05 \text{ m·s}^{-1} \leqq U \leqq 1 \text{ m·s}^{-1}$ (2-21)

         $7.0 \times 10^{-4} \text{ m} \leqq \delta \leqq 1.01 \times 10^{-3} \text{ m}$ (2-22)

         $3.6 \times 10^{-4} \text{ m} \leqq d_p \leqq 1.1 \times 10^{-3} \text{ m}$ (2-23)

         $0° \leqq \beta \leqq 65°$ (2-24)

If $d_p = 3.6 \times 10^{-4}$ m, $\delta = 2.5 \times 10^{-3}$ m, U = 0.1 m·s^{-1}
and $\beta = 65°$ for example, $U^{0.8} = 0.16$ and $3.5 U_B^{0.45} = 1.19$
in Eq.(2-16). So it is found that the effect of the
movement of particles over the clearance by the agitator
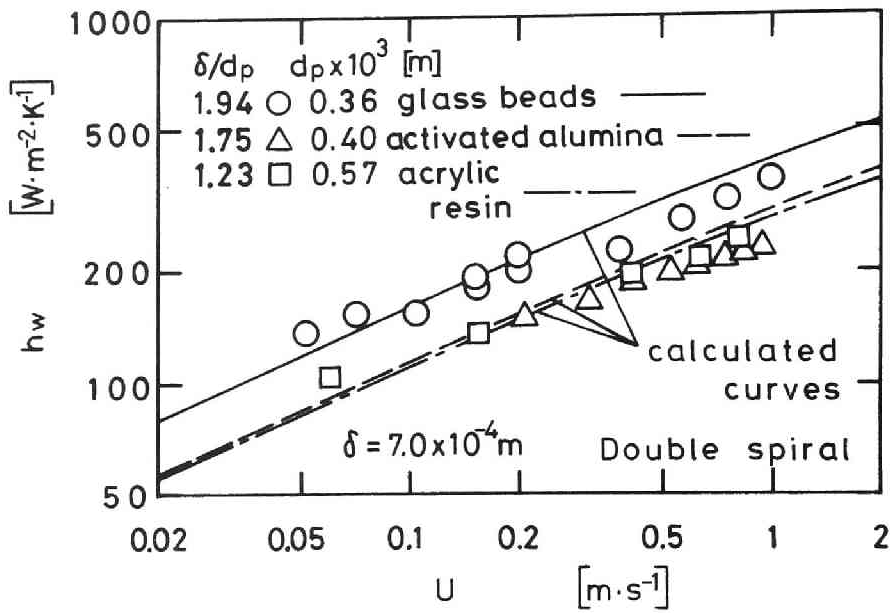blade is more than that of the circumferential velocity

Fig.2-7　Heat transfer coefficient vs. circumferential velocity of double spiral agitator
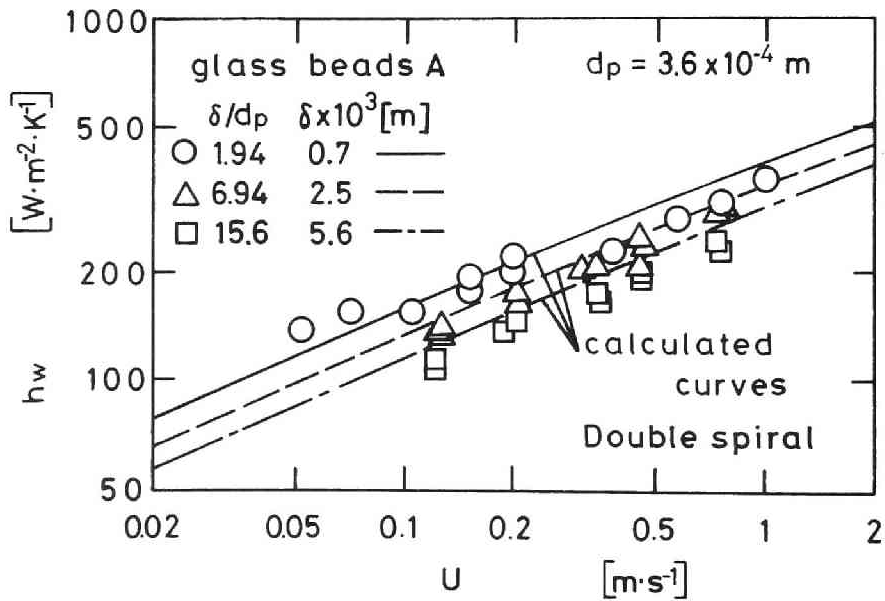

Fig.2-8　Heat transfer coefficient vs. circumferential velocity of double spiral agitator
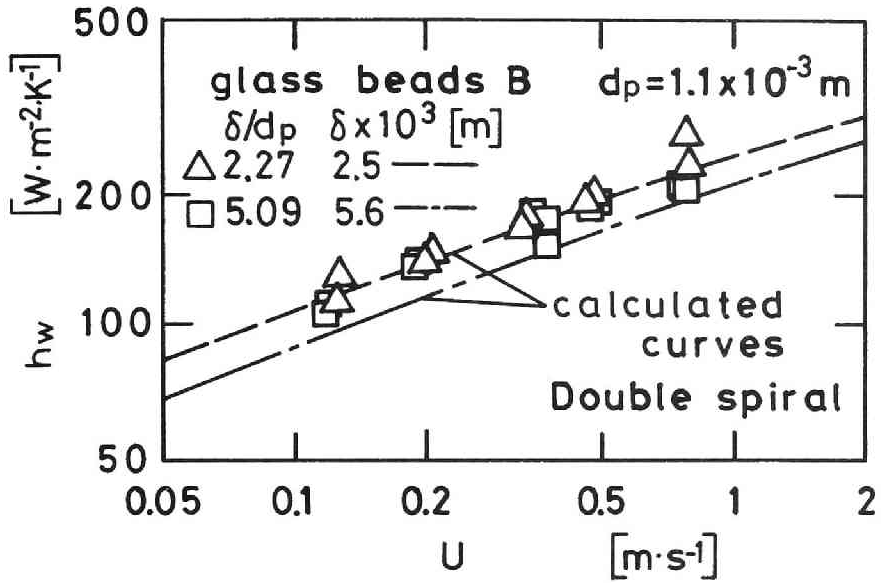
Fig.2-9   Heat transfer coefficient vs. circumferential
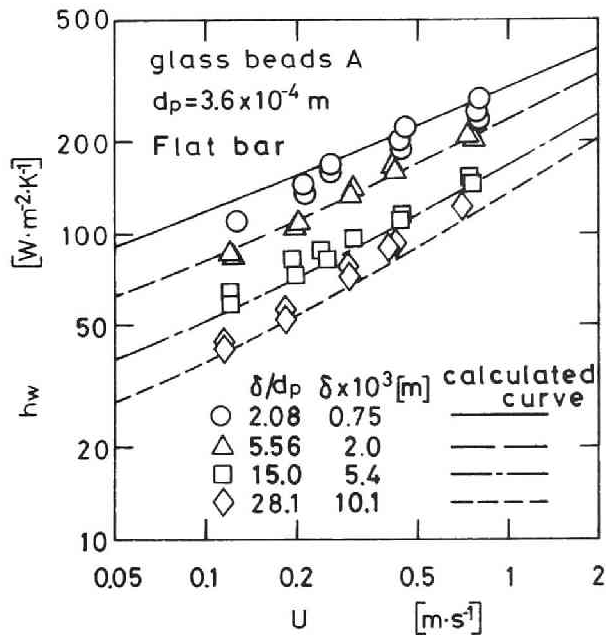velocity of double spiral agitator

Fig.2-10   Heat transfer coefficient vs. circumferential
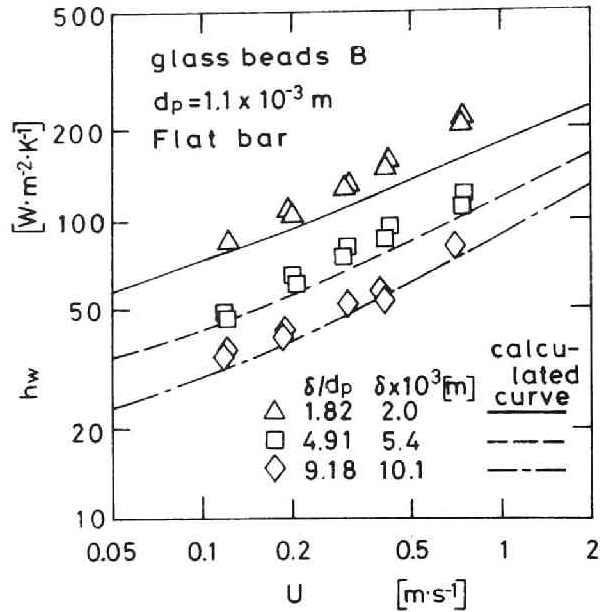velocity of flat bar agitator

Fig.2-11 Heat transfer coefficient vs. circumferential
velocity of flat bar agitator

of the agitator. Under this condition, the effective
thickness of the stationary particle layer δ_e is calcu-
lated to be equal to 3.38×10^{-4} m. This is about one
eighth of the width of the clearance.

In order to illustrate the effect of the clearance
on the heat transfer coefficient, the observed heat
transfer coefficients for $U = 0.2$ m·s^{-1} and $U = 0.8$ m·s^{-1}
are plotted as a function of the dimensionless clearance
δ/d_p in Figs.2-12 and 2-13. As shown in these figures,
the calculated heat transfer coefficient is constant
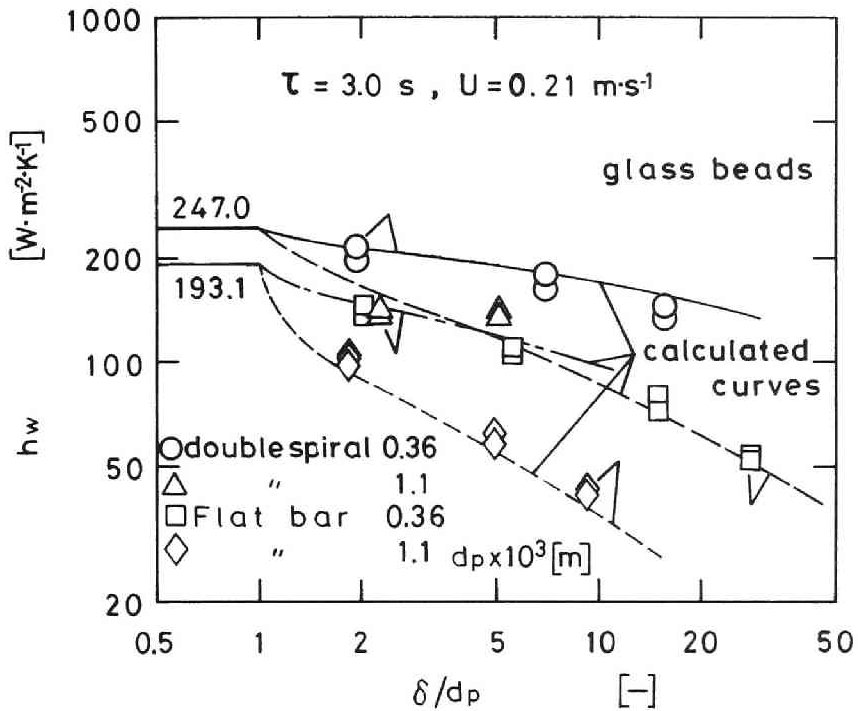when δ/d_p is less than unity. Then the calculated h_W

Fig.2-12 Heat transfer coefficient vs. dimensionless
          clearance

decreases with the increase of δ/d_p if δ/d_p is greater

than unity. The way of decrease has the following char-

acteristics:

1) h_w decreases rapidly if δ/d_p is near to unity

2) h_w decreases moderately in the region of δ/d_p =
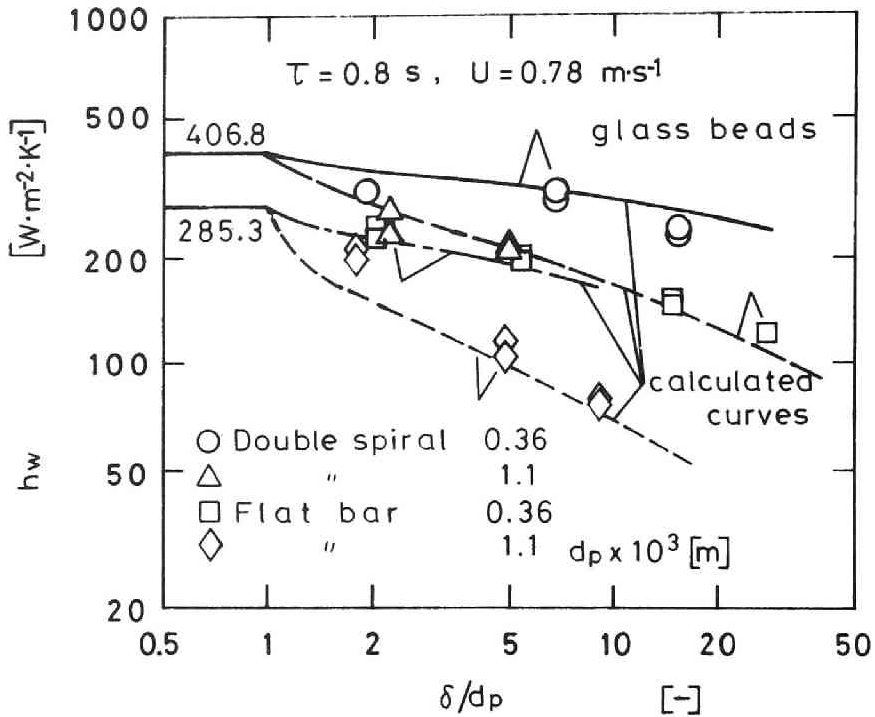
   2 ∿ 10.

Fig.2-13 Heat transfer coefficient vs. dimensionless
          clearance

3) the gradient of decrease is large again if δ/d_p is

   more than 10.

It is also shown in those figures that δ/d_p has a

greater influence on h_w in case of the flat bar agita-

tor than in case of the double spiral type. For the

different particle size and the circumferential veloc-
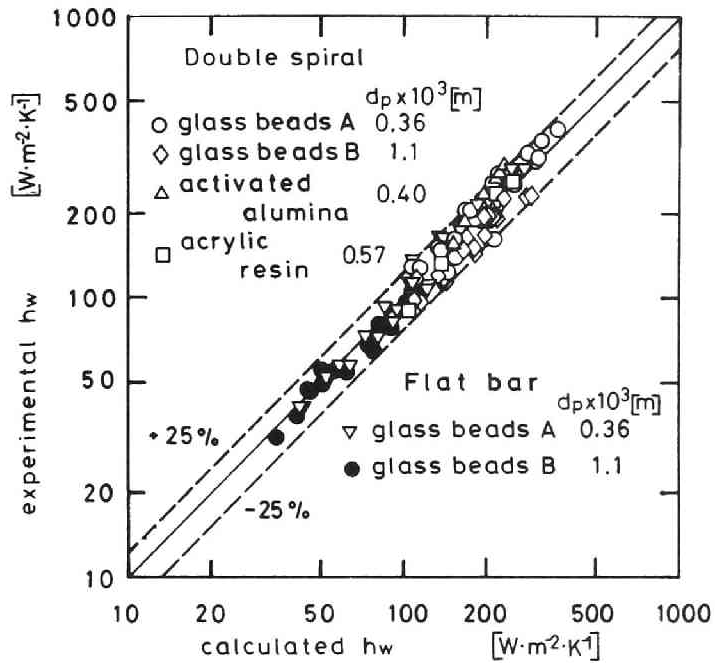
Fig.2-14 Experimental h_W vs. calculated h_W

ity of the agitator, the influence of δ/d_p and the effect of the type of the agitator on h_W are almost the same although the absolute values of h_W naturally have certain differences.

In Fig.2-14, the calculated h_W vs. the experimental h_W are shown for all data. As shown, all data are almost correlated within ±25%. Therefore, it is concluded that the agreement between the calculated and the experimental h_W is good under the condition that the shape of particle is spherical.
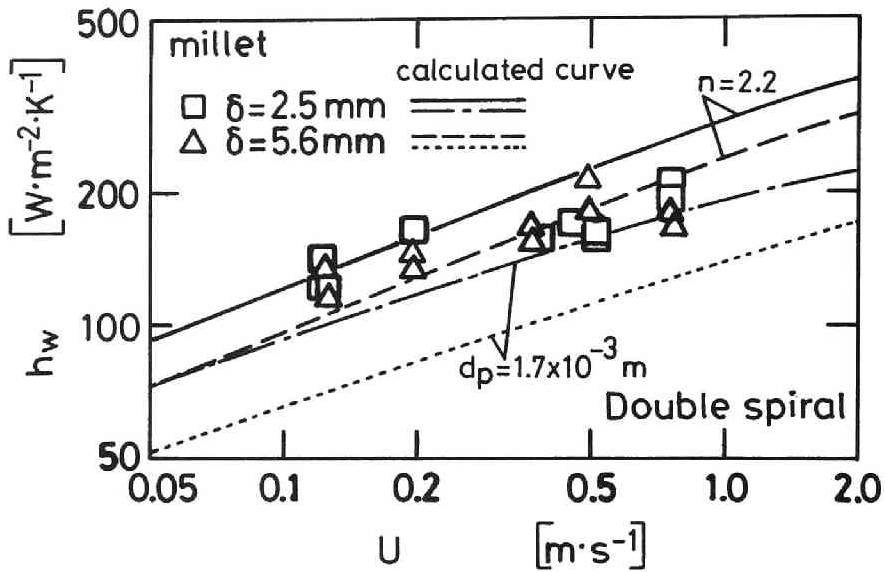
Fig.2-15   Heat transfer coefficient vs. circumferential
          velocity of double spiral agitator

Figure 2-15 shows h_w vs. U of double spiral agita-
tor for millet. As shown in Table 2-1, the shape of
millet is flat oval. Therefore, there is a serious de-
viation between the experimental and calculated heat
transfer coefficients when the average particle diameter
d_p = 1.7 mm, which was obtained by the sieving, was used
in the calculation of the wall-to-particle heat transfer
coefficient providing that its shape was spherical. The
wall-to-particle heat transfer coefficient naturally
depends on the shape of the particle. So it is neces-

Fig.2-16 Cross section of millet

sary to detrmine the shape of millet. Then we make the
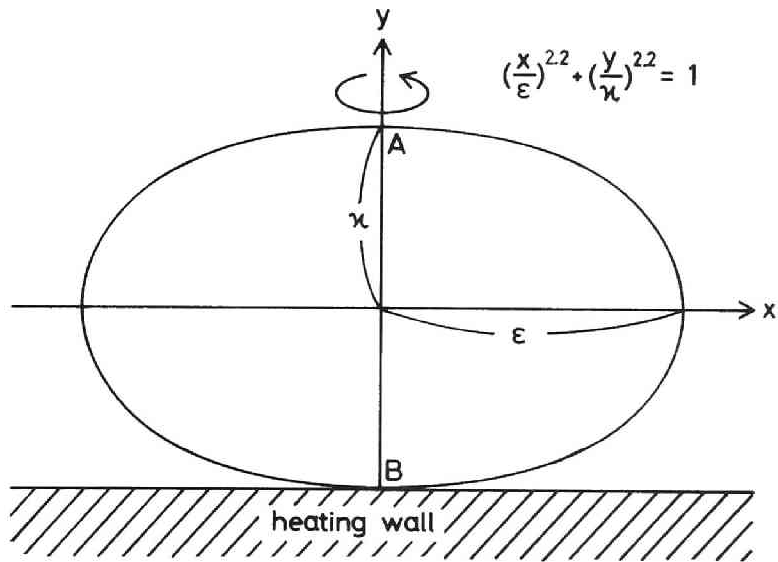following assumptions (Fig.2-16).

  (1) The cross section of millet is described by the
       following equation.

$$\left(\frac{x}{\varepsilon}\right)^n + \left(\frac{y}{\kappa}\right)^n = 1 \qquad (2-25)$$

  (2) The shape of millet is a rotation symmetry against
       the y-axis.

The parameter n in Eq.(2-25) was determined to be equal
to 2.2 by taking photographs of millet. In the calcu-
lation of δ_e, d_p = 1.01 mm was used, which was equal to
$\overline{AB}$ in Fig.2-16. The calculated curves obtained in this
way are also presented in Fig.2-15 and the comparison
between those and experimental data shows fairly good
agreement. Therefore, the present model can predict
the heat transfer coefficient in the case that the shape
of particle is not spherical if its shape can be ob-
tained quantitatively.

2-5 Conclusion

The heat transfer coefficient between the heating
wall and the mechanically agitated granular bed in the
small indirect-heat agitated dryer was measured. The
heat transfer model considering the effect of the clear-
ance between the heating wall and the agitator blades
was proposed. This model can describe the dependence of
the heat transfer coefficient on the circumferential
velocity of the agitator, the thermal properties of the
granular material, the particle size and the width of
the clearance. Furthermore, it was confirmed that this

model was still available in the case that the shape of particle was not spherical. Accordingly, by use of the present model, it is possible to estimate the heat transfer coefficient in the type of the indirect-heat agitated dryer used here.

CHAPTER 3

HEAT TRANSFER FROM SUBMERGED BODY MOVING IN GRANULAR
BED WITHOUT THROUGH-FLOW AIR

3-1 Introduction

The work described in this chapter is concerned
with the heat transfer in the "moving heating-plane
type" of the indirect-heat agitated dryer. In this
type, the agitator is hollow with a heating medium
flowing within it and the surface of the agitator acts
as a heating plane. The heating plane moves within
the granular bed. It is naturally expected that the
heat transfer coefficient in this type is higher than
that in the "stationary heating-plane type" because
there is not any clearance in the former. Furthermore,
the heat transfer area per dryer volume in this type can
be more than that in the "stationary heating-plane
type". Therefore, this type has been used in the large
indirect-heat agitated dryer.

There are generally two forms of the heating plane

in this type of the dryer: the rotating disk and the rotary coil. The former type has the week points that the construction is troublesome and that the weight is too heavy. On the other hand, it is expected that the latter type will be used widely because the construction is easy and the weight is light. However, there is also little information on the design of this type and few studies on the heat transfer between the "moving heating plane" and the granular bed have been reported.

The heat transfer in this case can be regarded as that between the granular bed and the body submerged in it under the condition that there exists the relative velocity between them. Then the heat transfer between the granular bed and the inclined heating cylinder submerged in it is dealt with in §3-2. After that, the heat transfer between the granular bed and the rotary coil, which is used actually in the dryer mentioned above, is dealt with in §3-3.

In order to measure the heat transfer coefficient in the former, the heat flux generator (H.F.G.) was used, which was especially prepared for this measurement by the author. Using this device, the heat transfer coefficient can be easily and quickly obtained.

3-2 Heating Cylinder

3-2-1 Theory and MOdel

It is considered that the heat transfer in this
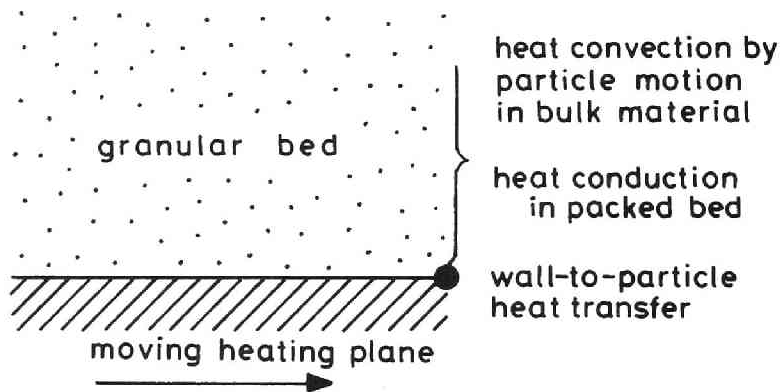case consists of three mechanisms as shown in Fig.3-1.

Fig.3-1 Heat transfer mechanism

1) wall-to-particle heat transfer

2) heat conduction in packed bed

3) heat convection by particle motion in bulk material

The heat convection by the particle motion in the bulk
material can be also neglected providing that it is

mixed perfectly. Therefore, the following equations can be also applied in this case as in §2-2.

$$h_p = 4(\lambda_g/d_p)\{(1 + 2\sigma/d_p)\ln(1 + d_p/2\sigma) - 1\} \qquad (2-1)$$

$$\sigma = 2\frac{2-\gamma}{\gamma} \sqrt{2\pi RT/M} \frac{\lambda_g}{p(2c_{pg} - R/M)} \qquad (2-2)$$

$$h_s = \psi h_p + (1 - \psi)h_{2p} + h_R \qquad (2-3)$$

$$h_c = \sqrt{\lambda_e c_{pm}\rho_b / \pi t} \qquad (2-9)$$

In this case, the heat transfer resistances are only two and so we can get the instantaneous heat transfer coefficient as follows when those resistances are connected in series to each other.

$$h_i = 1 / (1/h_s + 1/h_c) \qquad (3-1)$$

Accordingly, the time-averaged heat transfer coefficient can be obtained by integrating Eq.(3-1) during the contact time in this case after Eqs.(2-3) and (2-9) are substituted into Eq.(3-1).

$$h_{cy} = (\int_0^\tau h_i \, dt)/\tau = 2h_s\{\sqrt{\pi\tau^*} - \ln(1+\sqrt{\pi\tau^*})\}/(\pi\tau^*) \qquad (3-2)$$

$$\tau^* = h_s^2\tau/\lambda_e c_{pm}\rho_b \qquad (3-3)$$

In order to calculate the heat transfer coefficient using Eqs.(3-2) and (3-3), it is necessary to evaluate the contact time between the particles and the inclined heating cylinder. Therefore, we make the following assumptions to obtain the contact time.

(1) The particle flow near the cylinder wall is parallel to this wall and its velocity is constant and equal to that of bulk particles.

(2) There is no velocity distribution and no mixing of particles in the granular bed in the radial direction of the heating cylinder.

(3) Particles completely contact the semi-circle of the ellipse, which is the shape of the cross section of the heating cylinder when it is cut by the plane including the path-line of particles (Fig.3-2).

Under these assumptions, the contact time can be given by the following equations.

$$\tau = L / u_r \tag{3-4}$$

$$L = \frac{D_{cy}}{\sin\phi} \int_0^{\pi/2} \sqrt{1 - \cos^2\phi \sin^2\omega} \; d\omega \tag{3-5}$$
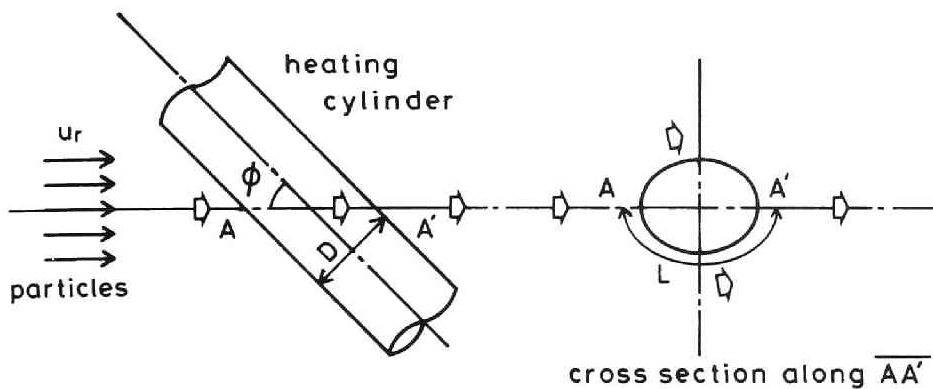
Fig.3-2 Motion of moving particles around inclined
cylinder

where D_{cy} is the diameter of the heating cylinder and
L is the contact length, which is equal to the semi-
circle of the ellipse as mentioned above.

Finally, the heat transfer coefficient in this case
can be calculated by Eqs.(2-1)∿(2-3) and (3-2)∿(3-5).

3-2-2 Experimentals

a)Apparatus

A schematic diagram of the experimental apparatus
is shown in Fig.3-3. The experiments were carried out
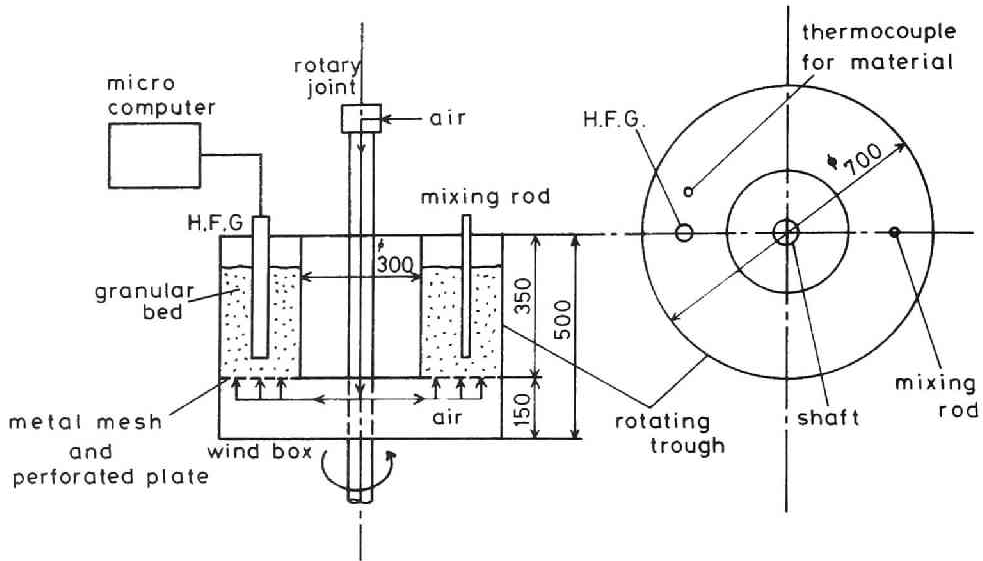
Fig.3-3 Schematic diagram of experimental apparatus

with a vertical double-cylindrical vessel. The outer
diameter is 70 cm and the inner one is 30 cm. The
height is 35 cm except for the wind box. The granular
material filled the annular space of the vessel. The
H.F.G. and the mixing rod were inserted into the bed
from the upper side as shown in Fig.3-3. The tempera-
ture of the granular bed was measured by the thermocouple
at about 10 cm ahead of the H.F.G..

In this apparatus, the granular bed is moving, while
the submerged heater is stationary. However, it can be
considered that this heat transfer coefficient is equal

to that in the case which the heating plane is moving in
the granular bed mixed perfectly.

The principle and the dimension of the H.F.G. is
shown in Fig.3-4. The surface temperature of the main
heater 1 was kept at constant by adjusting the electric
power. In order that heat generated in the main heater
may be transferred completely from its surface to the
granular bed, the guard heaters 2 and the devices for
measuring the temperature difference (D.M.T.D.) 4 are
installed at both ends of the main heater. Each guard
heater was controlled to keep the temperature difference
indicated by the corresponding D.M.T.D. equal to zero.
The D.M.T.D. consists of twelve thermocouples, by which
the electric power generated by the temperature differ-
ence of both sides of the D.M.T.D. is multiplied.

Two more heaters called the "dummy heater" 3 are
installed in the H.F.G.. These heaters prevent the
error caused by so-called the "entrance effect" from
getting into the measurement. When the angle between
the path-line of particles and the axis of the inclined
cylinder is small to some extent, the particle flowing
along the locus shown in Fig.3-5 reaches the main heater
with keeping the temperature of the bulk material unless

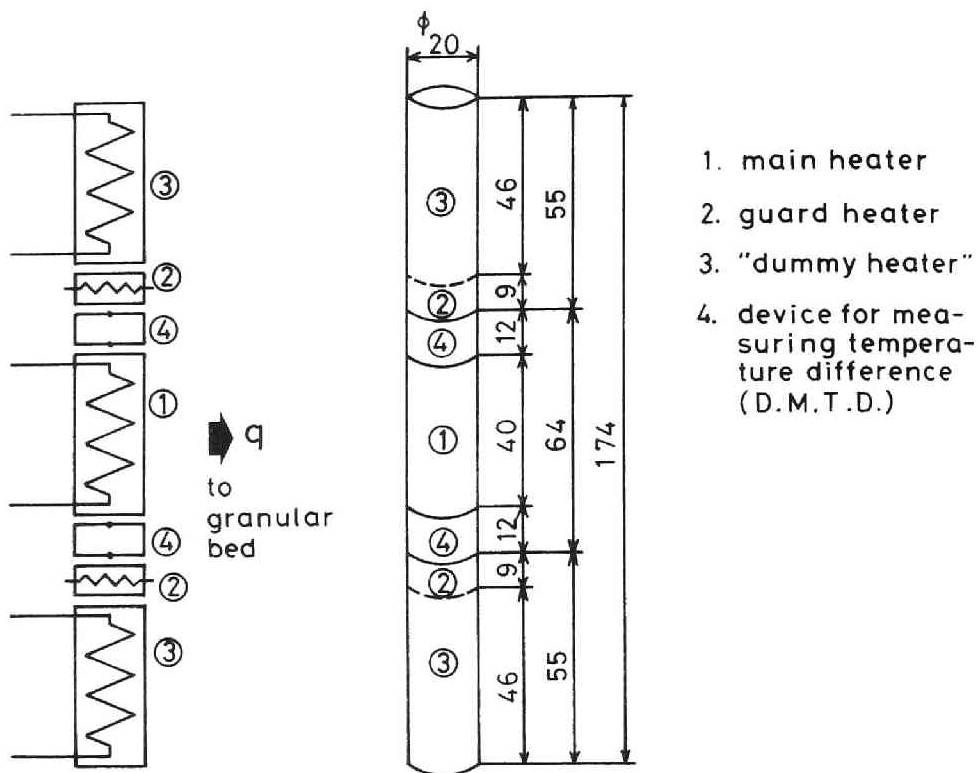Fig.3-4 Principle and dimension of heat flux generator
         (H.F.G.)

the "dummy heater" is installed. This causes the over-
estimation of the heat transfer coefficient. The sur-
face temperatures of these heaters were controlled to
keep them equal to that of the main heater. Each tem-
perature in the H.F.G. was measured by the thermocouple.
All heaters consisted of the nichrome wire were heated
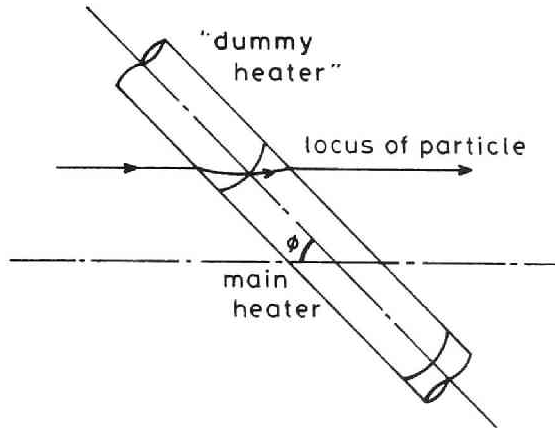
Fig.3-5   Entrance effect

electrically and controlled by the micro-computer.

The H.F.G. was calibrated by the experiment of the steady-state heat transfer to flowing water. As the result, the possible error by using the H.F.G. was estimated within 10%.

b) Procedure

All the experiments were carried out under the condition that the temperature of the heating plane was constant.

Using the H.F.G., the heat transfer coefficient can be calculated by the following equation as the electric

power put into the main heater is equal to the heat flux from the heater surface to the granular bed.

$$h_{cy} = q \, / \, \{A_{cy}(\, T_{cy} - T_b \,)\} \qquad (3\text{-}6)$$

After the granular material filled the annular space in the vessel, the rotational speed of the trough was set up a given one and the electric power was put into the main heater. After the surface temperature of the main heater reached a given one and the other heaters were controlled adequately, the change of the electric power and the temperature of the granular bed followed by the lapse of time were recorded. After that, the heat transfer coefficient was calculated by Eq.(3-6) using data obtained.

The possible overall error of the heat transfer coefficient introduced by the present experimental procedure is estimated at about 15%.

c) Granular materials

The glass beads was used for the present experiments. The properties are tabulated in Table 3-1. In

this table, the effective thermal conductivity of the granular bed was measured by the Q.T.M. rapid thermal conductivity meter (manufactured by Showa Denko Co., Ltd.; QTM-Dl) and the apparent density of the bed was also obtained by our measurement.

Table 3-1 Granular materials

Material	Shape	$d_p \times 10^3$ [m]	ρ_b [kg·m^{-3}]	c_{pm} [J·kg^{-1}·K^{-1}]	λ_e [W·m^{-1}·K^{-1}]
glass beads	sphere	0.36	1450	853	0.203

3-2-3 Results and Discussion

In Figs.3-6∿3-8, the observed heat transfer coefficients are plotted as a function of the relative velocity between the heating cylinder and the granular bed. The curves given in the same figures are calculated by the present model.

In the case of $\phi = 90°$ and $\phi = 135°$ (Figs.3-6 and 3-8), the agreement between the experimental and calcu-

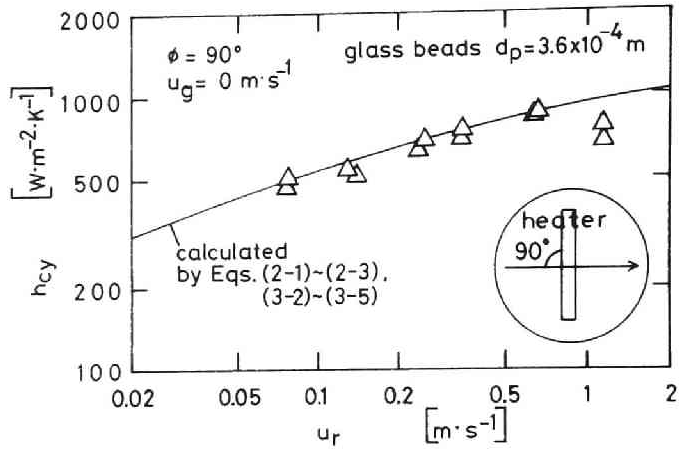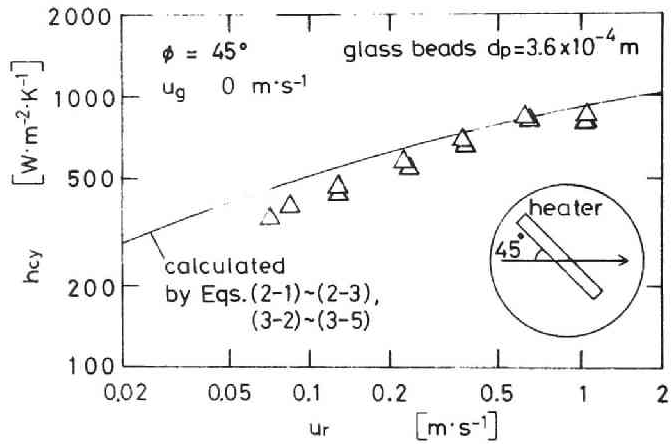Fig.3-6 h_{cy} vs. u_r with no through-flow air ($\phi = 90°$)

Fig.3-7 h_{cy} vs. u_r with no through-flow air ($\phi = 45°$)

2000

$\phi = 135°$ glass beads $d_P = 3.6 \times 10^{-4}$ m

$u_g = 0$ m·s^{-1}

$[W \cdot m^{-2} \cdot K^{-1}]$

1000

500

h_{cy} 200

calculated
by Eqs. (2-1)~(2-3),
(3-2)~(3-5)

heater
135°

100

0.02   0.05   0.1   0.2   0.5   1   2

u_r $[m \cdot s^{-1}]$
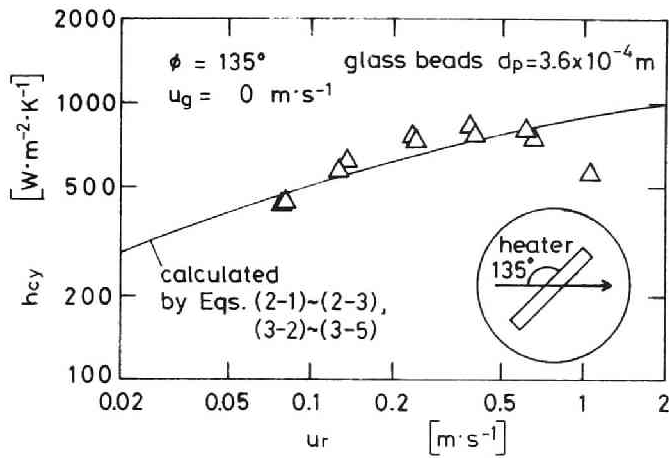
Fig.3-8 h_{cy} vs. u_r with no through-flow air ($\phi = 135°$)

lated heat transfer coefficients was fairly good so long as u_r is less than about 0.8 m·s^{-1}. However, the experimental data are located below the calculated curves in the range that u_r is more than about 0.8 m·s^{-1}. This can be explained by the fact that an air pocket was observed behind the cylinder in this range. It is considered that the air pocket causes the heat transfer area to decrease and therefore the heat transfer from the heating surface to the granular bed is also decreased. If it is possible to estimate the real heat transfer area, the experimental data in this range would also coincide with the calculated ones.

In the case of $\phi = 45°$ (Fig.3-7), the deviation in the range mentioned above is small as the size of the air pocket might be small even if it existed. On the contrary, the observed data are located a little below the calculated curve. It is considered that this is caused by the fact that the contact length was extended by that the path-line of particles turned to the bottom along the cylinder. Though it is thought that path-line of particles might also turn to the surface of the bed in the case of $\phi = 135°$, such a deviation did not appear in that case (Fig.3-8). This may be explained by the influence of the gravity force.

3-3 Rotary Coil

3-3-1 Theory and Model

As mentioned in §3-2-1, the following equations can also be used to calculate the heat transfer coefficient in this case.

$$h_{rc} = 2h_s\{\sqrt{\pi\tau^*} - \ln(1 + \sqrt{\pi\tau^*})\}/(\pi\tau^*) \qquad (3-7)$$

$$\tau^* = h_s^2\tau/\lambda_e c_{pm}\rho_b \qquad (3-3)$$

$$h_p = 4(\lambda_g/d_p)\{(1 + 2\sigma/d_p)\ln(1 + d_p/2\sigma) - 1\} \qquad (2-1)$$

$$\sigma = 2\frac{2-\gamma}{\gamma} \sqrt{2\pi RT/M} \; \frac{\lambda_g}{p(2c_{pg} - R/M)} \qquad (2-2)$$

$$h_s = \psi h_p + (1 - \psi)h_{2p} + h_R \qquad (2-3)$$

Fig.3-9   Contact between material and coil
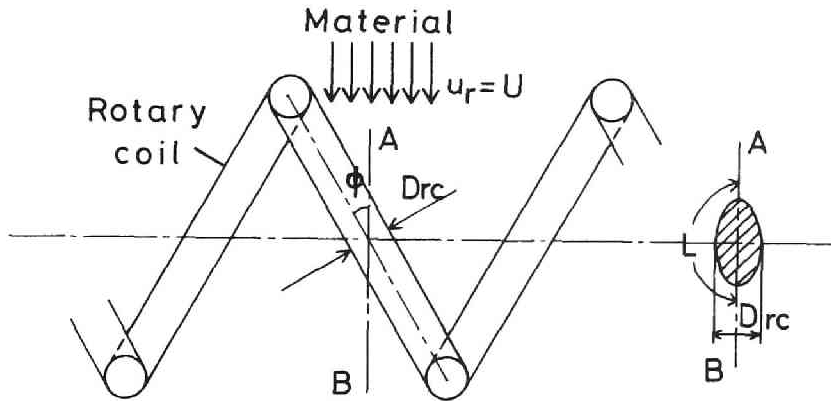
Furthermore, it is necessary to know the contact time. So we make the following assumptions (Fig.3-9):

(1) The direction of movement of particles in direct contact with the coil surface intersects with the axis of the coil at the angle ϕ.

(2) The relative velocity between particles and the rotary coil u_r is equal to the circumferential velocity of the rotary coil U.

Under these assumptions, the contact time can be given by the following same equations as those in the heating cylinder.

$$\tau = L / U \qquad\qquad (3-8)$$

$$L = \frac{D_{rc}}{\sin\phi} \int_{0}^{\pi/2} \sqrt{1 - \cos^2\phi\sin^2\omega} \; d\omega \qquad (3-9)$$

where D_{rc} is the diameter of the coil and L is the contact length, which is equal to the semi-circle of the ellipse. Finally, the heat transfer coefficient in this case can be calculated by Eqs.(2-1)∿(2-3), (3-3) and (3-7)∿(3-9).

3-3-2 Experimentals

 a) Apparatus

A schematic diagram of the experimental apparatus is shown in Fig.3-10. The experiments were carried out with the same small horizontal semi-cylindrical in-direct-heat agitated dryer as used in the Chapter 2. The details of the apparatus are described in §2-3.
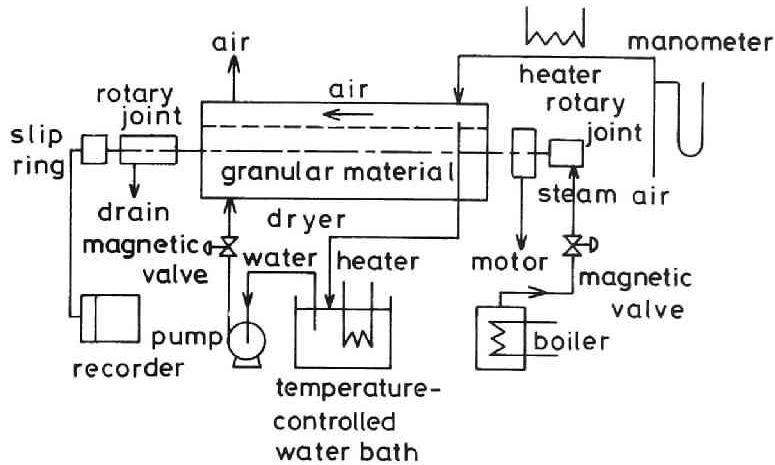
Fig.3-10 Schematic diagram of experimental apparatus

To avoid the heat transfers from the granular bed to the wall of the dryer and to air over the bed surface, hot water was circulated in the jacket and hot air was blown over the bed surface. Heaters for both water and air were controlled to keep the temperatures of both water and air equal to that of the granular bed.

The rotary coil used as the "moving heating plane type" of agitator is shown in Fig.3-11. The diameter of the coil was 2 cm, which was the same as the heating cylinder used in §3-2. To heat the coil surface, the steam was flowed within the hollow coil from one end and the drain was removed at the other end. The temperature of the coil surface was controlled by adjusting the
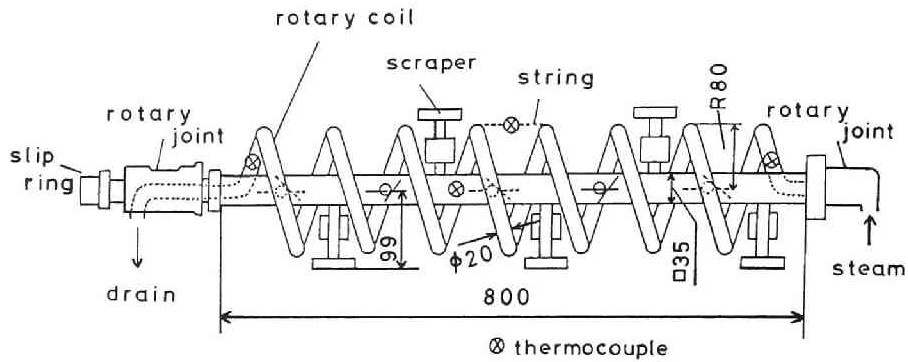
Fig. 3-11　Rotary coil

steam flow rate. It had been certified in advance that no temperature distrubution existed on the coil surface.

b) Procedure

All the experiments were also carried out under the condition that the temperature of the heating plane was constant.

The following equation can be obtained by the heat-balance in the system of both the granular bed and the agitator.

$$W_m c_{pm} \frac{dT_b}{dt} + W_{sh} c_{psh} \frac{dT_{sh}}{dt} = h_{rc} A_{rc} (T_{rc} - T_b) - h_w A_w (T_b - T_w)$$
$$- h_a A_a (T_b - T_a) - Q_{loss} \qquad (3-10)$$

- 56 -

where the first term on the left side is the heat accu-
mulation rate of the granular bed, the second is that of
the agitator, the first term on the right side is the
heat transfer rate from the rotary coil to the granular
bed, the second is that from the bed to the wall, the
third is that from the bed to air over the bed surface
and the fourth is other overall heat loss.

As mentioned above, T_w and T_a were equal to T_b in
the present experimental condition. So the second and
the third terms on the left side of Eq.(3-10) could be
deleted. Furthermore, the fourth term Q_{loss} was known
to be negligible compared with the first as the result
of the steady-state heat transfer experiment. Finally,
the time-averaged heat transfer coefficient can be cal-
culated by the following.

$$h_{rc} = (W_m c_{pm}\frac{dT_b}{dt} + W_{sh} c_{psh}\frac{dT_{sh}}{dt})/\{A_{rc}(T_{rc}-T_b)\} \qquad (3-11)$$

The hold-up of the material was about 60%. Be-
cause, the bulk material could not be mixed perfectly if
the hold-up was 100%. Accordingly, the heat transfer
area A_{rc} was not equal to all the coil surface. A part
of it was always exposed to air over the bed surface.

So the photographs were taken of the coil and A_{rc} was determined.

After the dryer was filled with materials, the rotary coil was heated up to a given temperature by blowing steam into the coil and the rotational speed of the rotary coil was set for a given one. Simultaneously, the flow of hot water and air was started. Then the changes of the temperatures of the granular bed and the shaft of the rotary coil followed by the lapse of time were recorded. After that, the heat transfer coefficient was calculated by Eq.(3-11) using data obtained.

The possible overall error of the heat transfer coefficient introduced by the present experimental procedure is estimated at about 15%.

c) Granular materials

Three kinds of granular materials were used for the present experiments. Two of them were glass beads A and B, which had the same thermal properties and only differed in the particle size. The other was a spherical activated alumina. The properties of these granular materials are tabulated in Table 3-2.

Table 3-2   Granular materials

Material	Shape	$d_p \times 10^3$	ρ_b	c_{pm}	λ_e
		[m]	[kg·m^{-3}]	[J·kg^{-1}·K^{-1}]	[W·m^{-1}·K^{-1}]
glass beads A	sphere	0.36	1450	853	0.203
glass beads B	sphere	1.1	1450	853	0.203
activated alumina	sphere	o.51	910	920	0.157

3-3-3   Results and Discussion

In Fig.3-12, h_{rc} vs. U is shown for the two sizes
of glass beads and the activated alumina. h_{rc} increases
as U increases for the glass beads A and the activated
alumina.   While h_{rc} for the glass beads B is almost con-
stant in the range: U = 0.1 ∿ 1 m·s^{-1}.   These phenomena
can be easily understood with an aid of Fig.3-13, where
the wall-to-particle heat transfer coefficient h_p and
the averaged heat transfer coefficient of the heat con-
duction in packed bed h_{cave} are shown for the glass beads
A and B. h_{cave} is obtained by integrating Eq.(2-9)
during the contact time.
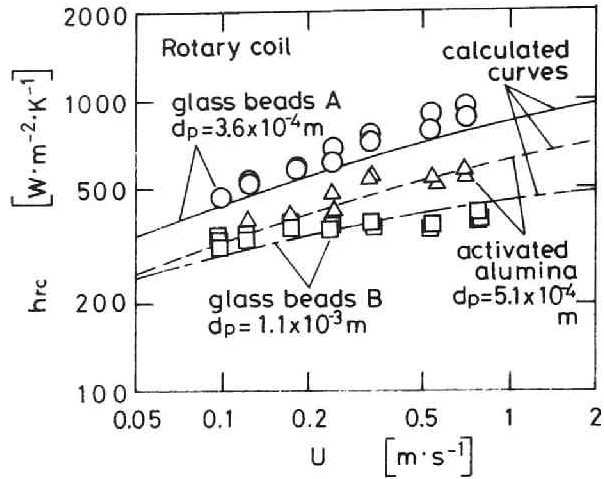
Fig.3-12 Heat transfer coefficient vs. circumferential
          velocity of rotary coil

$$h_{cave} = (\int_0^{\pi/2} h_c \, dt) / \tau$$
$$= 2 \sqrt{\lambda_e c_{pm} \rho_b / \pi\tau} \qquad (3\text{-}12)$$

where τ can be obtained by Eqs.(3-8) and (3-9).

As shown in Fig.3-13, the glass beads B is mainly
controlled by the wall-to-particle heat transfer resist-
ance, while the glass beads A are done by both the wall-
to-particle heat transfer resistance and the resistance
of the heat conduction in the packed bed. Many inves-
tigator have discussed about the effect of the contact
time or the circumferential velocity of the agitator on
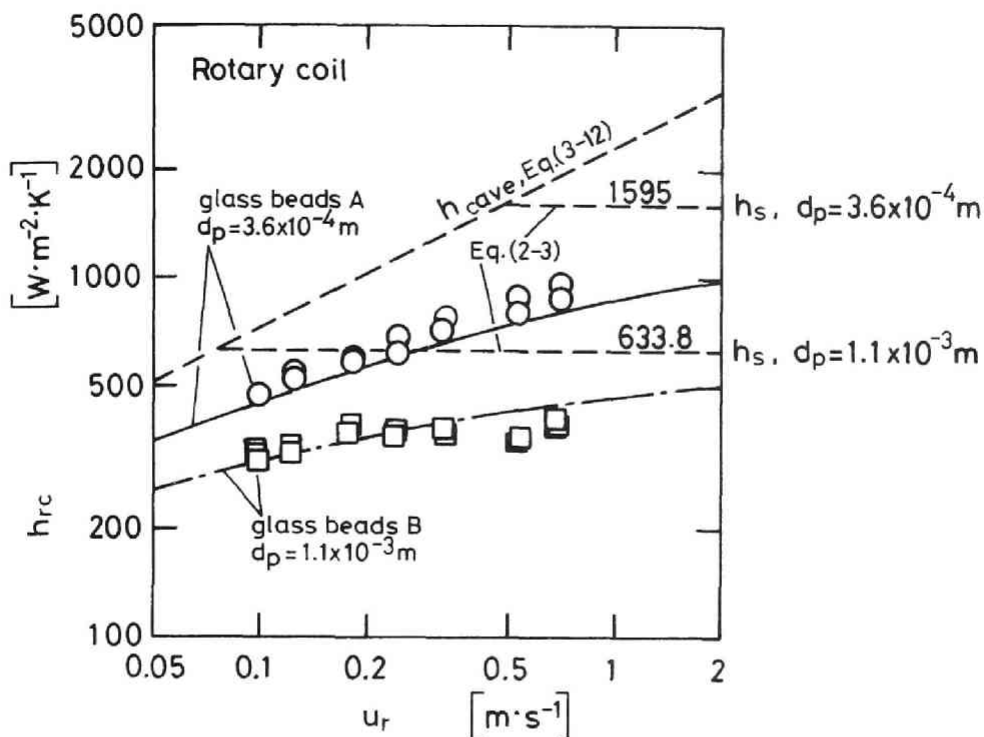
Fig.3-13 Comparison between calculated and experimental
h_{rc} for glass beads

the heat transfer coefficient. However, the present

model can perfectly describe this effect.

In Fig.3-12, the calculated curves by the present

model are also given. The experimental data of each

material agree with the respective calculated curves.

Therefore, it is thought that an air pocket did not

exist behind the coil in this case. After all, it is

concluded that the present model can describe the dependence of the heat transfer coefficient on the circumferential velocity of the rotary coil, the particle diameter and the thermal properties of granular material in the range of the experimental data considered.

3-4 Conclusion

The heat transfer coefficient between the granular bed and the heating cylinder submerged in it was measured under the condition that there existed the relative velocity between them. In order to measure the heat transfer coefficient in this case, the heat flux generator (H.F.G.) was used, which was made sure that the heat transfer coefficient was easily and quickly obtained with good accuracy.

The heat transfer coefficient between the granular bed and the rotary coil, which was used in the actual dryer and whose diameter was the same as that of the heating cylinder mentioned above, was measured.

The heat transfer model predicting the heat transfer coefficient between the "moving heating plane" and the granular bed was proposed. The comparison between

the observed and calculated heat transfer coefficients in both type of the "moving heating plane" showed fairly good agreement under the condition that an air pocket did not appear behind the heating cylinder. Accordingly, using the present model, it is possible to estimate the heat transfer coefficient in the type of the indirect-heat agitated dryer used here.

CHAPTER 4

HEAT TRANSFER FROM SUBMERGED BODY MOVING IN GRANULAR

BED WITH THROUGH-FLOW AIR

4-1   Introduction

One of the most serious problems of the large in-
direct-heat agitated dryer is that the power consump-
tion required for revolving the heating and agitating
devices is very large. Blowing gas through the granu-
lar bed is suggested as one method solving this and the
author found that a little through-flow gas decreased
the power consumption considerably described in §4-2.
This can be explained by that the cohesion among par-
ticle is decreased.

The through-flow gas also promotes the removal of
the vapor generated in the granular bed, which is so
effective on the drying of an adsorptive material and
a deliquescent crystals and it also promotes the mixing
of the bulk material. However, the velocity of this
through-flow gas must be less than the minimum fluidi-

zation one because the advantage that the exhaust gas is little in this type of dryer is lost and the power consumption of the blower becomes large. The overall power consumption must be less than that of the fluidized bed dryer or that of the agitated dryer without the device for the through-flow gas.

The work described in this chapter is concerned with the heat transfer in the new type of dryer which is the "moving heating-plane type" of the indirect-heat agitated dryer installed the device for the through-flow gas. This type is expected to have high performance and the present work will contribute to the development of this new type of dryer as its fundamentals.

About the heat transfer between the granular bed and the body submerged in it, many studies have been made so far mentioned in §1-1. However, few studies on the heat transfer in the state mentioned above have been reported. So this chapter concerns with the heat transfer in the flowing granular bed with the through-flow gas whose velocity is less than the minimum fluidization one in other words.

In order to measure the heat transfer coefficient in this case, the heat flux generator (H.F.G.) was also

used, which was the same as used in the Chapter 3.

4-2 Power Consumption

4-2-1 Experimentals

The experiments were carried out with a small hor-
izontal semi-cylindrical dryer, which was made of a
transparent acrylic resin plate in order to observe the
movement of particles. Its length is 27 cm and the di-
ameter is 26 cm. A schematic diagram of the experimen-
tal apparatus is shown in Fig.4-1.

The agitator used here was the flat bar type as
shown in the same figure. The torque for the agitation
of the material was measured by the Dynamic-static
torque meter (manufactured by Ono Sokki Co., Ltd.;
KST-5).

After the granular material filled the dryer, air
was blown into the bed at a given flow rate. Then the
rotational speed of the agitator was set up a given one
and the torque was measured by the torque meter.

Three kinds of granular materials were used for
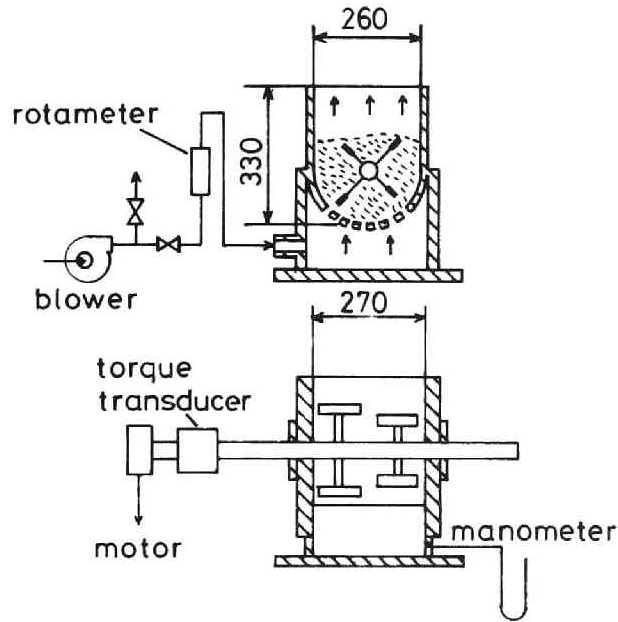this measurement. The properties of them are tabulated
in Table 4-1.

Fig.4-1 Schematic diagram of experimental apparatus

Table 4-1 Granular materials

Material	Shape	$d_p \times 10^3$ [m]	ρ_b [kg·m^{-3}]	u_{mf} [m·s^{-1}]
maltose A	irregular	0.57	490	0.1
maltose B	irregular	1.3	450	0.4
millet	flat oval	1.7	820	0.2

4-2-2 Results and Discussion
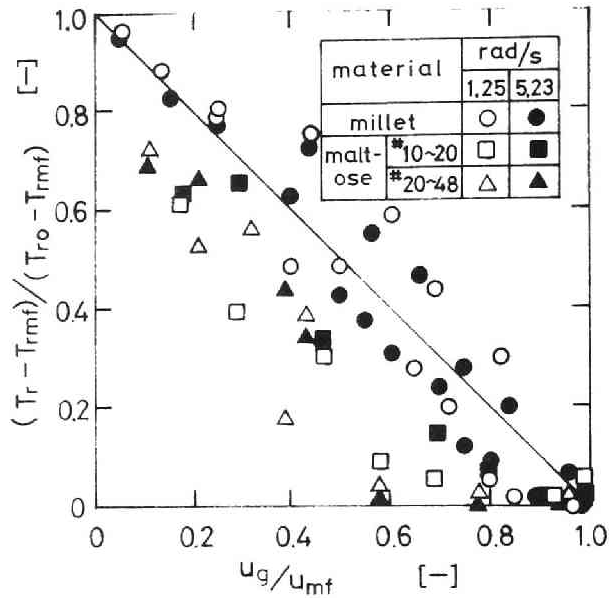
Fig.4-2 Dimensionless torque vs. dimensionless
velocity of through-flow air

In Fig.4-2, the dimensionless torques are plotted
as a function of the dimensionless velocity of the
through-flow air. As shown, those data are a little
scattered. However, we can find a qualitative result;
the torque for maltose, which is cohesive, can be reduced
with smaller amount of the through-flow air than that for
millet, which is free flowing. This phenomenon can be

explained that the through-flow air weakens the cohesion among particles.

It is necessary to investigate further the relation between the decrease of the power consumption and the properties of particle.

4-3 Theory and Model

The model described in §3-2-1 can be also applied in this case. So the following equations can be also used to calculate the heat transfer coefficient.

$$h_{cy} = 2h_s\{\sqrt{\pi\tau^*} - \ln(1 + \sqrt{\pi\tau^*})\} / (\pi\tau^*) \qquad (3\text{-}2)$$

$$\tau^* = h_s^2\tau/\lambda e c_{pm}\rho_b \qquad (3\text{-}3) \qquad \tau = L / u_r \qquad (3\text{-}4)$$

$$L = \frac{D_{cy}}{\sin\phi} \int_0^{\pi/2}\sqrt{1 - \cos^2\phi\sin^2\omega}\ d\omega \qquad (3\text{-}5)$$

$$h_p = 4(\lambda g/d_p)\{(1 + 2\sigma/d_p)\ln(1 + d_p/2\sigma) - 1\} \qquad (2\text{-}1)$$

$$\sigma = 2\frac{2-\gamma}{\gamma}\ \sqrt{2\pi RT/M}\ \frac{\lambda g}{p(2c_{pg} - R/M)} \qquad (2\text{-}2)$$

$$h_s = \psi h_p + (1 - \psi)h_{2p} + h_R \qquad (2\text{-}3)$$

Since the velocity of the through-flow gas is low, the temperature of the gas becomes that of the granular bed at once when it is led to the bed. Therefore, it is considered that the through-flow gas has the influence only on the effective thermal conductivity of the granular bed in the heat transfer in this case. This value can be predicted by the following equation proposed by Yagi and Kunii [29].

$$\frac{\lambda_e}{\lambda_g} = \frac{\lambda_e \, u_g=0}{\lambda_g} + (\alpha\zeta)(\frac{c_{pg}\eta_g}{\lambda_g})(\frac{d_p G}{\eta_g}) \qquad (4\text{-}1)$$

where α and ζ are dimensionless parameters depending on the state of packing of particles. When particles are arranged in the closest packing, $\alpha = 0.179$ and $\zeta = 1$.

Finally, the heat transfer coefficient in this case can be calculated by Eq.(2-1)$\sim$(2-3), (3-2)$\sim$(3-5) and (4-1).

4-4 Experimentals

The experimental apparatus and procedure were almost the same as those mentioned in §3-2-2. A schematic diagram of the experimental apparatus is shown in Fig.4-3.
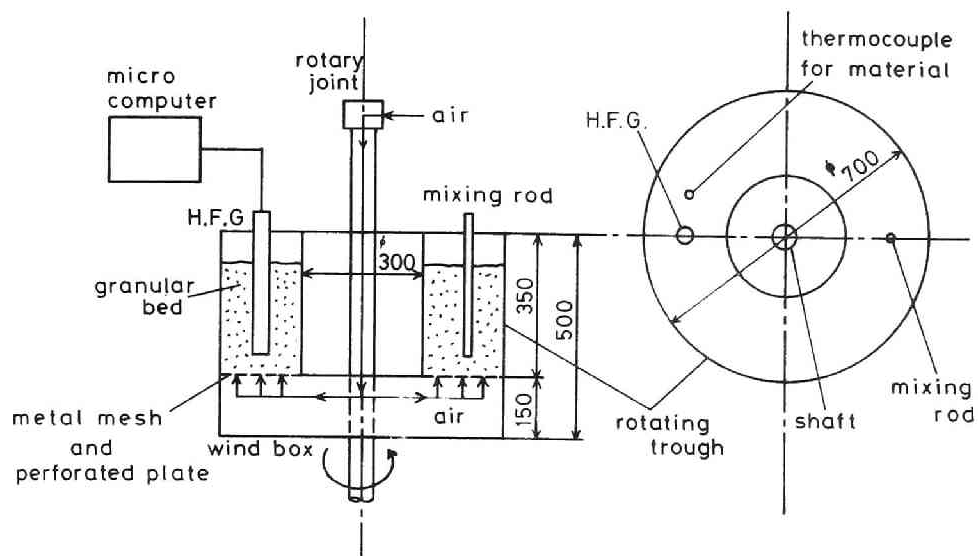
Fig.4-3 Schematic diagram of experimental apparatus

(This is the same figure as Fig.3-3.) The details of
this are described in §3-2. Air was led to the wind box
installed in the lower part of the vessel through the
rotary joint and the center hollow shaft. The perfo-
rated plate and the metal mesh were held between the
main body of the vessel and the wind box.

Using the H.F.G., whose details are described in
§3-3-2, the heat transfer coefficient can be calculated
by the following equation.

$$h_{cy} = q \ / \ \{A_{cy}(T_{cy} - T_b)\} \tag{3-6}$$

After the granular material filled the annular
space in the vessel, air was blown into the bed at a
given flow rate. Then the rotational speed of the
vessel was set up a given one and the electric power was
put into the main heater. After the surface temperature
of the main heater reached a given one and the other
heaters were controlled adequately, the change of the
electric power and the temperature of the granular bed
followed by the lapse of time were recorded. After that,
the heat transfer coefficient was calculated by Eq.(3-6)
using data obtained.

The possible overall error of the heat transfer co-
efficient introduced by the present experimental pro-
cedure is also estimated at about 15%

The glass beads was used as the granular material
for the present experiments. The properties are tabu-
lated in Table 4-2.

Table 4-2 Granular materials

Material	Shape	$d_p \times 10^3$ [m]	ρ_b [kg·m^{-3}]	c_{pm} [J·kg^{-1}·K^{-1}]	λ_e [W·m^{-1}·K^{-1}]
glass beads	sphere	0.36	1450	853	0.203

4-5 Results and Discussion

The minimum fluidization velocity u_{mf} was determined to be equal to 0.148 $m \cdot s^{-1}$ experimentally in this case. The heat transfer coefficients are plotted as a function of the relative velocity between the heating cylinder and the granular bed under the condition that $\phi = 90°$ and $u_g = 0.14$ $m \cdot s^{-1}$ in Fig.4-4. This velocity was a little less than the minimum fluidization one. The curve given in the same figure was calculated by the present model. The tendency of the agreement between the observed and calculated h_{cy} was the same as that in Fig.3-6. But, the air pocket appeared when u_r was more than about 0.5 $m \cdot s^{-1}$. This can be explained by that the through-flow air promotes the appearance of the air pocket. In Fig.4-5, h_{cy} vs. u_r is shown in the case of $\phi = 45°$ and $u_g = 0.14$ $m \cdot s^{-1}$. As shown, the observed data are scattered when u_r is larger than 0.2 $m \cdot s^{-1}$. This was caused by the fact that the state of the granular bed near the cylinder was unstable. So the discussion is limited to less than $u_r = 0.2$ $m \cdot s^{-1}$ in the following.
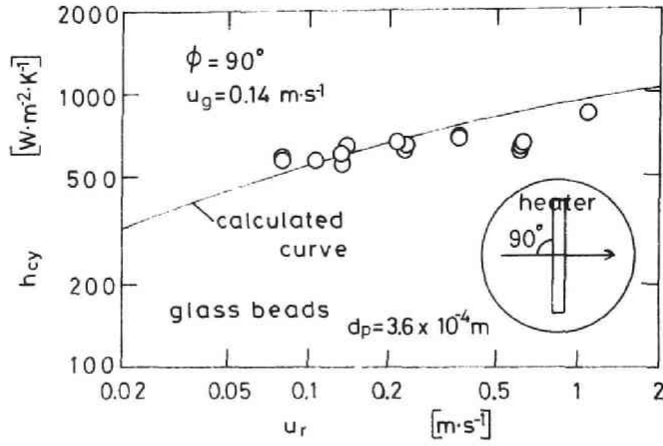
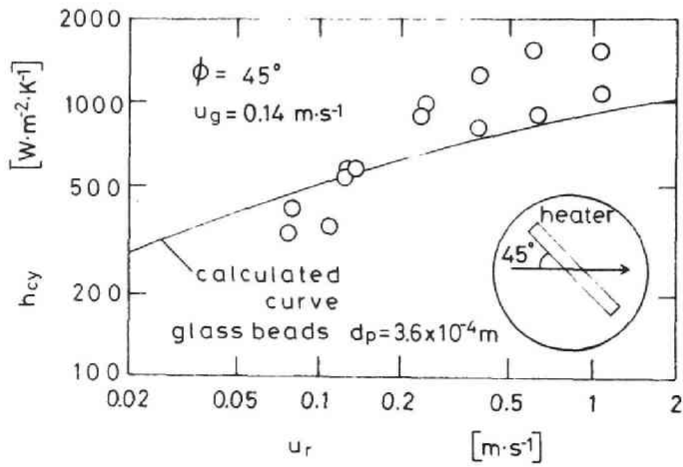Fig.4-4 h_c vs. u_r with through-flow air ($\phi = 90°$)

Fig.4-5 h_c vs. u_r with through-flow air ($\phi = 45°$)

In Figs. 4-6~4-8, the heat transfer coefficients are plotted as a function of the velocity of the through-flow air. On these figures are given the results calculated by the present model. Those lines are nearly flat and the experimental data are not also affected by the through-flow air in the range that its velocity is less than u_{mf}.

As known in Eq. (4-1), the effective thermal conductivity of the granular bed with the through-flow gas mainly depends on the velocity of it and the particle diameter and the minimum fluidization velocity also depend on the particle diameter. Therefore, it might be thought that the effect of the through-flow air is little because the particle diameter used here is small and that the larger the particle size is, the larger its effect on the heat transfer is. However, the wall-to-particle heat transfer resistance $1/h_s$, which is independent of the effective thermal conductivity of the bed, would be dominant in Eq. (3-1) in the case that the particle diameter is large unless u_r is so small. So, it is supposed that the effect of the through-flow gas on the heat transfer is also insignificant in the range that the particle size is large if u_r is not so small.
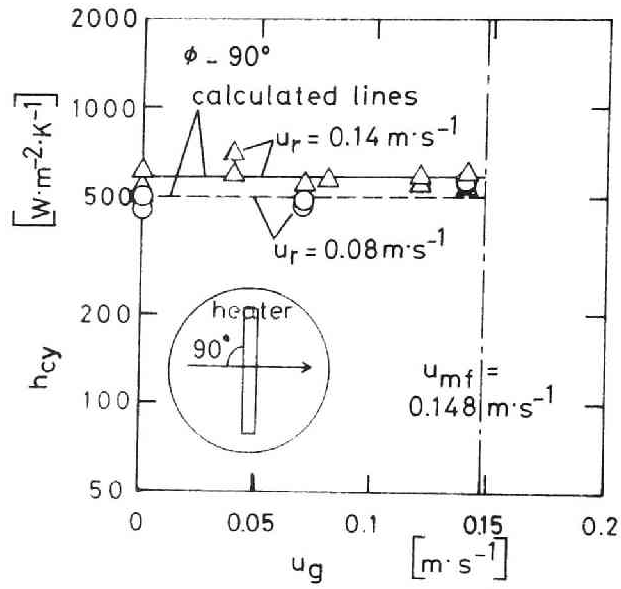
Fig.4-6 h_C vs. u_g ($\phi = 90°$)
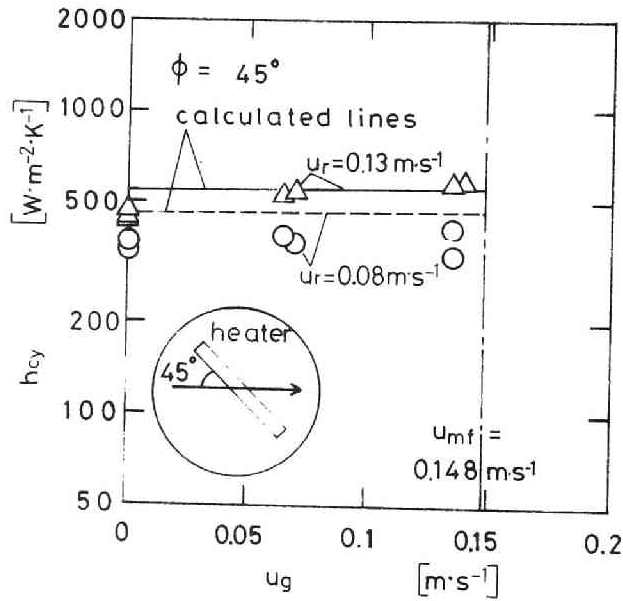
Fig.4-7 h_C vs. u_g ($\phi = 45°$)
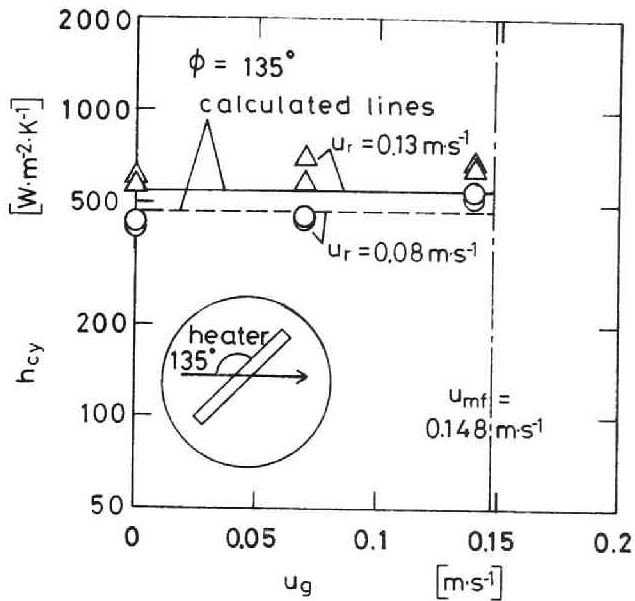
Fig.4-8   h$_C$ vs. u$_g$ (ϕ = 135°)

4-6   Conclusion

The heat transfer coefficient between the granular
bed and the heating cylinder submerged in it was mea-
sured under the condition that there existed the rela-
tive velocity between them and that air flowed through
the bed.   The velocity of the through-flow air was
limited to less than the minimum fluidization velocity.
The heat flux generator (H.F.G.) was used in order to
measure the heat transfer coefficient.

The heat transfer model considering the effect of the through-flow gas was proposed. The agreement between the observed and calculated heat transfer coefficients was fairly good.

As the result of this work, it is concluded that the effect of the through-flow gas on the heat transfer coefficient is insignificant providing that its velocity is less than the minimum fluidization velocity and that the relative velocity between the cylinder and the granular bed is not so small. This result is useful in the development of the new dryer; the "moving heating-plane type" of the indirect-heat agitated dryer installed the device for the through-flow gas.

CHAPTER 5

CONCLUSION AND PROBLEMS IN FUTURE WORKS

5-1 Conclusions

The heat transfer between the heating plane and the granular bed in the indirect-heat agitated dryer was investigated experimentally and theoretically.

CHAPTER 2

The heat transfer coefficient between the heating wall and the mechanically agitated granular bed in the "stationary heating-plane type" of the indirect-heat agitated dryer was measured. The heat transfer model considering the effect of the clearance between the heating wall and the agitator blades was proposed. This model can describe the dependence of the heat transfer coefficient on the circumferential velocity of the agitator, the thermal properties of the granular material, the particle size and the width of the clearance.

Furthermore, it was confirmed that this model was

available even in the case that the shape of particle was not spherical. Accordingly, by use of the present model, it is possible to estimate the heat transfer coefficient in the "stationary heating-plane type" of the indirect-heat agitated dryer used here.

CHAPTER 3

The heat transfer coefficient between the granular bed and the inclined heating cylinder submerged in it was measured under the condition that there existed the relative velocity between them. In order to measure the heat transfer coefficient in this case, the heat flux generator (H.F.G.) was used, which was especially prepared for this measurement by the author and which was made sure that the heat transfer coefficient was easily and quickly obtained with good accuracy.

The heat transfer coefficient between the granular bed and the rotary coil, which used in the actual "moving heating-plane type" of the indirect-heat agitated dryer and whose diameter was the same as that of the heating cylinder mentioned above, was measured.

The heat transfer model predicting the heat transfer coefficient between the "moving heating plane" and

the granular bed was proposed. The comparison between
the observed and calculated heat transfer coefficients
in both type of the "moving heating plane" showed fairly
good agreement under the condition that an air pocket
did not appear behind the heating cylinder. Therefore,
using the present model, it is possible to estimate the
heat transfer coefficient in the "moving heating-plane
type" of the indirect-heat agitated dryer used here.

CHAPTER 4

As it was found that the power consumption required
for the agitation of the material was decreased by
blowing little gas through the granular bed, the devel-
opment of the "moving heating-plane type" of the in-
direct-heat agitated dryer combined with the device for
the through-flow gas was considered.

In order to obtain the fundamental data of this new
type of dryer, the heat transfer coefficient between the
granular bed and the heating cylinder submerged in it
was measured under the condition that there existed the
relative velocity between them and that air flowed
through the bed. The velocity of through-flow air was
limited to less than the minimum fluidization velocity.

The heat flux generator (H.F.G.) was also used in order to measure the heat transfer coefficient in this case.

The heat transfer model considering the effect of the through-flow gas was proposed. The agreement between the observed and calculated heat transfer coefficient was fairly good. As the result of this work, it was concluded that the effect of the through-flow gas on the heat transfer coefficient was insignificant providing that its velocity was less than the minimum fluidization velocity and that the relative velocity between the heating cylinder and the granular bed was not so small. This result is useful in the development of the new dryer; the "moving heating-plane type" of the indirect-heat agitated dryer installed the device for the through-flow gas.

5-2 Problems in Future Works

The problems in future works are considered to be as follows.

1) mixing degree of bulk material particles
2) effect of moisture content of granular bed

3) effect of diameter of dryer

4) effect of through-flow gas on performance of drying

5) modelling of drying mechanism in this type of dryer

These are related to each other.

1) mixing degree of bulk material particles

In this study, the effect of the mixing of bulk
material particles on the heat transfer was not con-
sidered and all the experiments were carried out under
the condition that the bulk material particles were
mixed perfectly. However, this is very important prob-
lem in the actual large dryer and it is thought that
this effect is significant. Although Schlünder intro-
duced the mixing number into his model as one method
solving this problem [20∿22, for example], the further
investigation should be proceeded.

2) effect of moisture content of granular bed

The particles including the equilibrium moisture
content were used in the present experiments. The pres-
ent model is only available when the fluidity of the
particle is good and agglomeration does not occur.
However, the material being treated in the actual dryer

includes the more moisture. The effect of the moisture content on the effective thermal conductivity of the granular bed can be estimated by the measurement or the several models [7,15, for example]. Besides the following problems remain in this field. The higher moisture content often causes particles to cohere the heating plane and this coherent particles from the heat transfer resistance on the heating plane. Further, we must consider the agglomeration which likely occurs at high moisture content. When agglomeration occurs, the mixing degree of the bulk material decreases and the apparent particle diameter increases. Therefore, it is naturally considered that the heat transfer coefficient decreases in that case.

3) effect of diameter of dryer

When the scale-up of the dryer is considered, this problem must be taken into account. Although this might have an effect only on the mixing of bulk material, few studies on this problem have been reported. So it is necessary to confirm it experimentally.

4) effect of through-flow gas on performance of drying

It was concluded that the effect of the through-flow gas on the heat transfer was insignificant. However, the through-flow gas has moreover the effects promoting the decrease of the power consumption, the removal of the vapor generated in the granular bed and the mixing of the bulk material as mentioned in §4-1. About the decrease of the power consumption, the experimental results were described in §4-2. However, it is necessary to investigate the relation between the decrease of the power consumption and the property of particle. About the removal of the vapor generated in the granular bed and the mixing of the bulk material, further investigations are also needed.

5) modelling of drying mechanism in this type of dryer

In order to evaluate the performance of the dryer, the drying rate must be discussed finally. It naturally depends on the type of dryer. Therefore, it is certainly necessary to establish the accurate model predicting the drying rate in this type of dryer.

NOMENCLATURE

A	area	$[m^2]$
a	constant in Eq.(2-16)	$[-]$
b	constant in Eq.(2-16)	$[-]$
c	constant in Eq.(2-16)	$[-]$
c_p	specific heat at constant pressure	$[J \cdot kg^{-1} \cdot K^{-1}]$
D	diameter of agitator	$[m]$
D_B	width of agitator blade	$[m]$
D_{cy}	diameter of heating cylinder	$[m]$
D_{rc}	diameter of rotary coil	$[m]$
D_t	thickness of agitator blade	$[m]$
d	constant in Eq.(2-16)	$[-]$
d_p	particle diameter	$[m]$
e	constant in Eq.(2-16)	$[-]$
G	mass flow rate	$[kg \cdot m^{-2} \cdot s^{-1}]$
h	heat transfer coefficient	$[W \cdot m^{-2} \cdot K^{-1}]$
L	contact-heating length	$[m]$
M	molar weight	$[kg \cdot kmol^{-1}]$
n	parameter in Eq.(2-25)	$[-]$
p	pressure	$[Pa]$
Q_{loss}	heat loss	$[W]$
q	heat flow	$[W]$

R	gas constant	$[J \cdot kmol^{-1} \cdot K^{-1}]$
T	temperature	$[K]$
T_r	torque	$[kg \cdot m]$
t	time	$[s]$
U	circumferential velocity of agitator	$[m \cdot s^{-1}]$
U_B	relative velocity between particle and agitator blade along lateral plane of blade shown in Eq.(2-17)	$[m \cdot s^{-1}]$
u_g	velocity of through-flow air	$[m \cdot s^{-1}]$
u_{mf}	minimum fluidization velocity	$[m \cdot s^{-1}]$
u_r	relative velocity between cylinder and granular bed	$[m \cdot s^{-1}]$
W	weight	$[kg]$
x	coordinates	$[-]$
y	coordinates	$[-]$
α	constant in Eq.(4-1)	$[-]$
β	angle of blade to moving direction of it	$[rad]$
γ	accomodation coefficient	$[-]$
δ	width of clearance between heating plane and agitator blade	$[m]$

δ_e	effective thickness of stationary particle layer on heating plane	[m]
ζ	constant in Eq.(4-1)	[-]
η	viscocity	$[kg \cdot m^{-1} \cdot s^{-1}]$
λ_e	effective thermal conductivity of granular bed	$[W \cdot m^{-1} \cdot K^{-1}]$
λ_g	thermal conductivity of gas	$[W \cdot m^{-1} \cdot K^{-1}]$
μ	angle of repose	[rad]
ξ	variable defined by Eq.(2-16)	[-]
ρ_b	apparent density of granular bed	$[kg \cdot m^{-3}]$
σ	modified mean free path of gas molecule defined by Eq.(2-2)	[-]
τ	contact time	[s]
τ°	modified contact time defined by Eq.(2-12)	[-]
τ^*	modified contact time defined by Eq.(3-3)	[-]
ϕ	angle between flow line of particles and axis of heating cylinder or rotary coil	[rad]
ψ	surface coverage factor	[-]

Subscripts

a   air over granular bed

B   agitator blade

b   granular bed

c   conduction

cy   cylinder

g   gas

i   instantaneous value

m   granular material

p   particle

R   radiation

r   relative value

rc   rotary coil

s   particle layer

sh   shaft of agitator

w   wall

LITERATURE CITED

1) Borodulya, V.A., V.L. Ganzha and A.I. Zheltov, Lett. Heat Mass Transfer, $\underline{7}$, 83 (1980)

2) Brinn, M.S., S.J. Friedman, F.A. Gluckert and R.L. Pigford, Ind. Eng. Chem., $\underline{40}$, 1050 (1948)

3) Ernst, R., Chem.-Ing.-Tech., $\underline{32}$, 17 (1960)

4) Gabor, J.D., Chem. Eng. Sci., $\underline{25}$, 979 (1970)

5) Harakas, N.K. and K.O. Beatty Jr., Chem. Eng. Prog. Symp. Ser., $\underline{59}$, No.41, 122 (1963)

6) Kharchenko, N.V. and K.E. Makhorin, Int. Chem. Eng., $\underline{4}$, 650 (1964)

7) Krischer, O. and H. Esdorn, VDI Forsch., $\underline{22}$, 1 (1956)

8) Krischer, O. and W. Kast, "Die wissenschaftlichen Grundlagen der Trocknungstechnik", 3rd ed., p117 Springer-Verlag, Berlin (1978)

9) Kurochkin, Yu.P., I. F. Zh., $\underline{2}$, 3 (1958)

10) Kurochkin. Yu.P., J. Eng. Phys., $\underline{10}$, 447 (1966)

11) Lehmberg, J., M. Hehl and K. Schugerl, Powder Tech., $\underline{18}$, 149 (1977)

12) Lücke, R., VT-Verfahrenstechnik, $\underline{10}$, 774 (1976)

13) Martin, H., Chem.-Ing.-Tech., $\underline{52}$, 199 (1980)

14) Mollekopf, N. and H. Martin, VT-Verfahrenstechnik, 16, 701 (1982)

15) Okazaki, M., I. Ito and R. Toei, AIChE Symp. Ser., 73, No.163, 164 (1977)

16) Perry, R.H. and C.H. Chilton, "Chemical Engineers' Handbook", 5th ed., p20-45, McGraw-Hill, New York (1973)

17) Reiter, T.W., J. Camposilvan and R. Nehren, Wärme-Stoffübertrag., 5, 116 (1972)

18) Schlünder, E.U., Chem.-Ing.-Tech., 43, 651 (1971)

19) Schlünder, E.U., Int. J. Heat Mass Transfer, 17, 1087 (1974)

20) Schlünder, E.U., VT-Verfahrenstechnik, 14, 459 (1980)

21) Schlünder, E.U., Chem.-Ing.-Tech., 53, 925 (1981)

22) Schlünder, E.U., Proc. 7th Int. Heat Transfer Conf., vol 1, 195 (1982)

23) Schlünder, E.U. and N. Mollekopf, Chem. Eng. Proces., 18, 93 (1984)

24) Schlünder, E.U., Chem. Eng. Proces., 18, 31 (1984)

25) Sullivan, W.N. and R.H. Sabersky, Int. J. Heat Mass Transfer, 18, 97 (1975)

26)   Uhl, V.W. and W.L. Root, Ⅲ, Chem. Eng. Prog.,
      63, 81 (1967)

27)   Wicke, E. and F. Fetting, Chem.-Ing.-Tech., 26,
      301 (1954)

28)   Wunschmann, J. and E.U. Schlünder, VT-
      Verfahrenstechnik, 9, 501 (1975)

29)   Yagi, S and D. Kunii, AIChE J., 3, 373 (1957)

30)   Yasutomi, T. and S. Yokota, Kagakukogaku
      Ronbunshu, 2, 205 (1976)